References

Aizawa H, Sawada J, Hideyama T, Yamashita T, Katayama T, Hasebe N, Kimura T, Yahara O, Kwak S (2010) TDP-43 pathology in sporadic ALS occurs in motor neurons lacking the RNA editing enzyme ADAR2. Acta Neuropathol 120: 75-84

Arai T, Hasegawa M, Akiyama H, Ikeda K, Nonaka T, Mori H, Mann D, Tsuchiya K, Yoshida M, Hashizume Y et al (2006) TDP-43 is a component of ubiquitin-positive tau-negative inclusions in frontotemporal lobar degeneration and amyotrophic lateral sclerosis. Biochem Biophys Res Commun 351: 602-611

Benkhelifa-Ziyyat S, Besse A, Roda M, Duque S, Astord S, Carcenac R, Marais T, Barkats M (2013) Intramuscular scAAV9-SMN injection mediates widespread gene delivery to the spinal cord and decreases disease severity in SMA mice. Mol Ther 21: 282-290

Bhalla T, Rosenthal JJ, Holmgren M, Reenan R (2004) Control of human potassium channel inactivation by editing of a small mRNA hairpin. Nat Struct Mol Biol 11: 950-956

Dayton RD, Wang DB, Klein RL (2012) The advent of AAV9 expands applications for brain and spinal cord gene delivery. Expert Opin Biol Ther 12: 757-766

Duque S, Joussemet B, Riviere C, Marais T, Dubreil L, Douar AM, Fyfe J, Moullier P, Colle MA, Barkats M (2009) Intravenous administration of self-complementary AAV9 enables transgene delivery to adult motor neurons. Mol Ther 17: 1187-1196

Foust KD, Nurre E, Montgomery CL, Hernandez A, Chan CM, Kaspar BK (2009) Intravascular AAV9 preferentially targets neonatal neurons and adult astrocytes. Nat Biotechnol 27: 59-65

Gao G, Vandenberghe LH, Alvira MR, Lu Y, Calcedo R, Zhou X, Wilson JM (2004) Clades of adeno-associated viruses are widely disseminated in human tissues. J Virol 78: 6381-6388

Hideyama T, Kwak S (2011) When does ALS start? ADAR2-GluA2 hypothesis for the etiology of sporadic ALS. Front Mol Neurosci 4: 33

Hideyama T, Yamashita T, Aizawa H, Tsuji S, Kakita A, Takahashi H, Kwak S (2012) Profound downregulation of the RNA editing enzyme ADAR2 in ALS spinal motor neurons. Neurobiol Dis 45: 1121-1128

Hideyama T, Yamashita T, Suzuki T, Tsuji S, Higuchi M, Seeburg PH, Takahashi R, Misawa H, Kwak S (2010) Induced loss of ADAR2 engenders slow death of motor neurons from Q/R site-unedited GluR2. J Neurosci 30: 11917-11925

Hwu WL, Muramatsu S, Tseng SH, Tzen KY, Lee NC, Chien YH, Snyder RO, Byrne BJ, Tai CH, Wu RM (2012) Gene therapy for aromatic ʟ-amino acid decarboxylase deficiency. Sci Transl Med 4: 134ra161

Iwata N, Sekiguchi M, Hattori Y, Takahashi A, Asai M, Ji B, Higuchi M, Staufenbiel M, Muramatsu S, Saido TC (2013) Global brain delivery of neprilysin gene by intravascular administration of AAV vector in mice. Sci Rep 3: 1472

Kawahara Y, Ito K, Sun H, Aizawa H, Kanazawa I, Kwak S (2004) Glutamate receptors: RNA editing and death of motor neurons. Nature 427: 801

Kawahara Y, Ito K, Sun H, Kanazawa I, Kwak S (2003) Low editing efficiency of GluR2 mRNA is associated with a low relative abundance of ADAR2 mRNA in white matter of normal human brain. Eur J Neurosci 18: 23-33

Kwak S, Kawahara Y (2005) Deficient RNA editing of GluR2 and neuronal death in amyotropic lateral sclerosis. J Mol Med 83: 110-120

Li XG, Okada T, Kodera M, Nara Y, Takino N, Muramatsu C, Ikeguchi K, Urano F, Ichinose H, Metzger D et al (2006) Viral-mediated temporally controlled dopamine production in a rat model of Parkinson disease. Mol Ther 13: 160-166

Lonergan T, Teschemacher AG, Hwang DY, Kim KS, Pickering AE, Kasparov S (2005) Targeting brain stem centers of cardiovascular control using adenoviral vectors: impact of promoters on transgene expression. Physiol Genomics 20: 165-172

Mingozzi F, High KA (2011) Therapeutic in vivo gene transfer for genetic disease using AAV: progress and challenges. Nat Rev Genet 12: 341-355

Nakamura T, Takumi T, Takano A, Aoyagi N, Yoshiuchi K, Struzik ZR, Yamamoto Y (2008) Of mice and men—universality and breakdown of behavioral organization. PLoS ONE 3: e2050

Neumann M, Sampathu DM, Kwong LK, Truax AC, Micsenyi MC, Chou TT, Bruce J, Schuck T, Grossman M, Clark CM et al (2006) Ubiquitinated TDP-43 in frontotemporal lobar degeneration and amyotrophic lateral sclerosis. Science 314: 130-133

Nishimoto Y, Yamashita T, Hideyama T, Tsuji S, Suzuki N, Kwak S (2008) Determination of editors at the novel A-to-I editing positions. Neurosci Res 61: 201-206

Petrs-Silva H, Dinculescu A, Li Q, Deng WT, Pang JJ, Min SH, Chiodo V, Neeley AW, Govindasamy L, Bennett A et al (2011) Novel properties of tyrosine-mutant AAV2 vectors in the mouse retina. Mol Ther 19: 293-301

Sawada J, Yamashita T, Aizawa H, Aburakawa Y, Hasebe N, Kwak S (2009) Effects of antidepressants on GluR2 Q/R site-RNA editing in modified HeLa cell line. Neurosci Res 64: 251-258

Singh M, Kesterson RA, Jacobs MM, Joers JM, Gore JC, Emeson RB (2007) Hyperphagia-mediated obesity in transgenic mice misexpressing the RNA-editing enzyme ADAR2. J Biol Chem 282: 22448-22459

Thevenot E, Jordao JF, O'Reilly MA, Markham K, Weng YQ, Foust KD, Kaspar BK, Hynynen K, Aubert I (2012) Targeted delivery of self-complementary adeno-associated virus serotype 9 to the brain, using magnetic resonance imaging-guided focused ultrasound. Hum Gene Ther 23: 1144-1155

Yamashita T, Hideyama T, Hachiga K, Teramoto S, Takano J, Iwata N, Saido TC, Kwak S (2012a) A role for calpain-dependent cleavage of TDP-43 in amyotrophic lateral sclerosis pathology. Nat Commun 3: 1307

Yamashita T, Hideyama T, Teramoto S, Kwak S (2012b) The abnormal processing of TDP-43 is not an upstream event of reduced ADAR2 activity in ALS motor neurons. Neurosci Res 73: 153-160

Yamashita T, Tadami C, Nishimoto Y, Hideyama T, Kimura D, Suzuki T, Kwak S (2012c) RNA editing of the Q/R site of GluA2 in different cultured cell lines that constitutively express different levels of RNA editing enzyme ADAR2. Neurosci Res 73: 42-48

ORIGINAL ARTICLE *Laboratory science*

Production of functional coagulation factor VIII from iPSCs using a lentiviral vector

Y. KASHIWAKURA,*† T. OHMORI,* J. MIMURO,* S. MADOIWA,* M. INOUE,‡
M. HASEGAWA,‡ K. OZAWA§ and Y. SAKATA*

*Research Division of Cell and Molecular Medicine, Center for Molecular Medicine, Jichi Medical University, Tochigi, Japan;
†Department of Immunology, Dokkyo Medical University School of Medicine, Tochigi, Japan; ‡DNAVEC Corporation,
Ibaraki, Japan; and §Division of Genetic Therapeutics, Center for Molecular Medicine, Jichi Medical University, Tochigi,
Japan

Summary. The use of induced pluripotent stem cells (iPSCs) as an autologous cell source has shed new light on cell replacement therapy with respect to the treatment of numerous hereditary disorders. We focused on the use of iPSCs for cell-based therapy of haemophilia. We generated iPSCs from mesenchymal stem cells that had been isolated from C57BL/6 mice. The mouse iPSCs were generated through the induction of four transcription factor genes Oct3/4, Klf-4, Sox-2 and c-Myc. The derived iPSCs released functional coagulation factor VIII (FVIII) following transduction with a simian immunodeficiency virus vector. The subcutaneous transplantation of iPSCs expressing FVIII

into nude mice resulted in teratoma formation, and significantly increased plasma levels of FVIII. The plasma concentration of FVIII was at levels appropriate for human therapy at 2–4 weeks post transplantation. Our data suggest that iPSCs could be an attractive and prospective autologous cell source for the production of coagulation factor, and that engineered iPSCs expressing coagulation factor might provide a cell-based therapeutic strategy appropriate for haemophilia.

Keywords: haemophilia, induced pluripotent stem cells, lentiviral vector, cell therapy, gene therapy, blood coagulation

Introduction

Haemophilia is an X-linked inherited bleeding disorder, caused by mutations within the *coagulation factor VIII* (*F8*) or *coagulation factor IX* (*F9*) genes. This results in a longer than average time for blood to clot, which can lead to significant bleeding. Haemophilia is considered suitable for gene therapy, as it is caused by a single gene abnormality, and therapeutic coagulation factor levels can vary across a broad range [1]. Recently, therapeutic levels of coagulation factor have been achieved in haemophilia B patients through the direct administration of adeno-associated virus vectors in clinical trials [2]. Another gene therapy strategy for haemophilia is the application of cells transduced *ex vivo*, as a delivery vehicle for coagulation factor [3].

Cell-based therapy reduces the risk of unwanted virus dissemination, and ensures the selection of highly expressing clones prior to commencement of the procedure. However, cell-based therapies for haemophilia have been hampered in animals and during human clinical trials, because of the short life span of transplanted cells, difficulties in obtaining therapeutic plasma levels, and elimination of the transduced cells by immune reactions [4].

Induced pluripotent stem cells (iPSCs) are artificially generated stem cells, made by reprogramming somatic cells through the expression of defined transcription factors [5,6]. These iPSCs are pluripotent, with the ability to differentiate into cells of the three germ lineages *in vitro*. Mouse-derived iPSCs can be passaged through the germ line, as is the case with embryonic stem cells (ESCs). Using iPSCs has a distinct advantage over ESCs, as cells differentiated from iPSCs exhibit limited immunogenicity, and are therefore more easily tolerated by a recipient following transplantation. Accordingly, iPSC technology offers the possibility of patient-specific cell therapy for haemophilia, in which the use of genetically identical cells would prevent immune rejection. In this study, we examined whether iPSCs could release

Correspondence: Tsukasa Ohmori, MD, PhD, Research Division of Cell and Molecular Medicine, Center for Molecular Medicine, Jichi Medical University, 3111-1 Yakushiji, Shimotsuke, Tochigi 329-0498, Japan.
Tel: +81-285-58-7397; fax: +81-285-44-7817;
e-mail: tohmori@jichi.ac.jp

functional coagulation factor using lentiviral transduction. We then focused on the possible clinical application of the engineered iPSCs to cell-based gene therapy for haemophilia.

Materials and methods

Mice

C57BL/6J mice were purchased from Japan SLC (Shizuoka, Japan). BALB/cAJcl-*nu/nu* mice (nude mice) were obtained from CLEA Japan, Inc. (Shizuoka, Japan). All animal procedures were approved by the Institutional Animal Care and Concern Committee at Jichi Medical University, and animal care was in accordance with the committee's guidelines.

Generation of iPSCs and cell culture

Murine mesenchymal stem cells (MSCs) were isolated and maintained as described previously [7]. We selected MSCs for the establishment of iPSCs because MSCs have a higher reprogramming efficiency compared with fibroblasts [8,9]. Two plasmid vectors to generate iPSCs (pCX-OKS-2A and pCX-cMyc) were obtained from Addgene (Cambridge, MA). MSCs were transduced with the plasmid vectors by nucleofection as described previously [10]. Colonies that were ES-like were cloned at 30 days post transduction, and MSC-derived iPSCs were maintained on mouse embryonic fibroblasts with knockout Dulbecco's modified Eagle's medium (DMEM; Invitrogen, Carlsbad, CA) supplemented with 15% foetal bovine serum, 2 mM L-glutamine, 1 mM sodium pyruvate, 0.1 mM non-essential amino acids, 0.5 mM monothioglycerol (Wako Pure Chemical Industries, Ltd., Osaka, Japan) and 1000 U mL^{-1} ESGRO (Merck Millipore, Billerica, MA).

Reverse transcription polymerase chain reaction (RT-PCR)

Total RNA was prepared using an RNeasy Mini Kit (QIAGEN, Montgomery, MD). The RT-PCR assays were conducted using a SuperScript One-Step RT-PCR System (Invitrogen). Primer pairs for the RT-PCR assays used in this study have been previously reported [5].

Lentiviral vector construct and production

The cDNA for human B-domain-deleted FVIII (hBDD-FVIII) was generated as previously described [11]. The *hBDD-FVIII* gene, under the control of a chicken β-actin promoter coupled with cytomegalovirus promoter early enhancer element (CAGp), was cloned into a self-inactivating simian immunodeficiency virus (SIV) lentiviral vector [12]. The SIV lentiviral vectors were generated as previously described [13].

Measurement of FVIII activity and antigen

The hFVIII antigens (FVIII:Ag) were measured using an anti-hFVIII-specific enzyme-linked immunosorbent assay (ELISA) kit (ASSERACHROM VIII:Ag; Diagnostica Stago, Seine, France). The functional activity of FVIII (FVIII:C) was measured using a one-stage clotting time assay on an automated coagulation analyser (Sysmex CA-500 analyser; Sysmex Corp., Kobe, Japan). We used pooled normal human plasma as a reference to measure both FVIII:C and FVIII:Ag.

Results and discussion

We first attempted to establish iPSCs from C57BL/6 mice. Bone marrow-derived MSCs were transduced with plasmid vector expressing the defined transcription factors. We cloned ESC-like cell colonies after transduction, and SSEA-1 positive cells were sorted by flow cytometry (Fig. 1a). The sorted cell colonies exhibited typical ESC morphology and alkaline phosphatase activity (Fig. 1b). The mRNA expression patterns of endogenous pluripotent-specific genes (*Sox2, Oct3/4, Nanog* and *c-Myc*) in the cells were similar to those in E14tg2a mouse ESCs (Fig. 1c). Furthermore, subcutaneous transplantation of these cells (1 × 10^6 cells) into nude mice resulted in the formation of teratomas containing tissues derived from the ectoderm, mesoderm, and endoderm (Fig. 1d and e). This would suggest that the cells possess the potential to differentiate into cells and tissues of the three germ layers. Therefore, we used these iPSCs for further experiments in this study.

We next examined whether iPSCs could produce functional coagulation factor after transduction by a lentiviral vector. The iPSCs were transduced with the SIV vector expressing hBDD-FVIII under the control of CAGp (SIV-CAG-hFVIII) (Fig. 2a). We cloned iPSC colonies from the cells transduced with SIV-CAG-hFVIII at a multiplicity of infection (MOI) of 30, and selected three iPSC clones that stably produced hFVIII in the supernatant (Fig. 2b). The iPSC clones expressing hFVIII were subcutaneously transplanted into nude mice. Following transplantation, plasma levels of hFVIII:Ag in nude mice gradually increased according to teratoma formation derived from the transplanted iPSCs (Fig. 2c and d). Although the plasma level of hFVIII:Ag in the nude mice was at 20%, we could not measure hFVIII:C in nude mice because of the existence of mouse FVIII. We simultaneously measured hFVIII:C and hFVIII:Ag produced from transduced
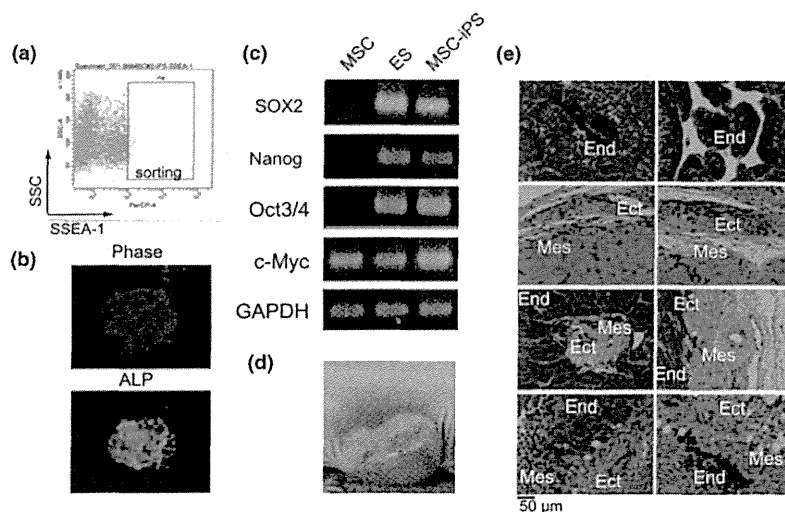
Fig. 1. Characterization of induced pluripotent stem cells (iPSCs) derived from mesenchymal stem cells (MSCs). MSCs isolated from C57BL/6 mice were transduced with plasmid vectors expressing Oc3/4, Klf4, Sox2 and c-Myc. (a) Stage-specific embryonic antigen 1 (SSEA-1) expression was examined by flow cytometry following transduction. SSEA-1-positive cells (shown in the square) were sorted as MSC-derived iPSCs. (b) Morphology of iPSC colonies derived from SSEA-1-positive cells. Alkaline phosphatase activity in iPSC colonies was detected using HNP/Fast Red TR. (c) The mRNA expression levels of the pluri-potency markers SOX2, Nanog, Oct3/4 and c-Myc were determined by reverse transcription polymerase chain reaction. (d) Teratoma formation in nude mice after subcutaneous transplantation of iPSCs. (e) Differentiation into cells and tissues of the three germ lineages were confirmed by histological analysis. End, endoderm; Ect, ectoderm; Mes, mesoderm.

iPSCs, and calculated the ratio of hFVIII:C to hFVIII: Ag (0.30 ± 0.041). Accordingly, hFVIII:C levels seemed to reach the therapeutic level of FVIII required for haemophilia A (6%) in transplanted mice.

Recent studies have reported the potential of iPSCs for the treatment of many human diseases; iPSCs possess the ability to differentiate into cardiovascular [14–16], haematopoietic [16,17], neural [18], and hepatic [19,20] progenitor cells. Treatment of inherited disorders using iPSCs has been proposed for animal models of sickle cell anaemia [17]. The haemophilic mouse model could also be used to examine the potential of iPSC therapy. Xu *et al.* reported that transplantation of endothelial progenitor cells derived from iPSCs into the liver increased FVIII levels, resulting in a corrected bleeding phenotype for haemophilia A mice [21,22]. The results reported by Xu *et al.* were surprising because the differentiated endothelial progenitor cells that were transplanted only contained one copy of *F8*, yet they were able to increase plasma levels of FVIII. In contrast, lentiviral transduction using our procedure resulted in 5–10 proviral integration sites in the diploid genome at an MOI of 30, suggesting that the same procedure using engineered iPSCs expressing coagulation factor would result in a more potent therapeutic effect.

In our preliminary experiments, we used nude mice to verify the following: the net production of FVIII from iPSCs by excluding the role of the immune system; and pluripotency of iPSCs by teratoma formation. However, tumourigenesis by iPSCs, should be
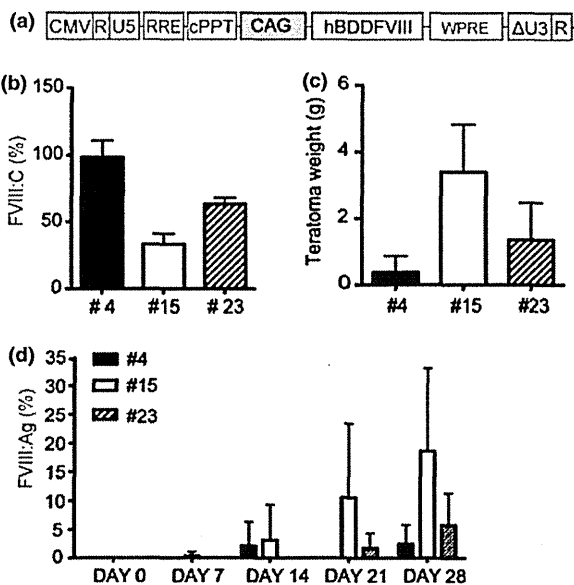
Fig. 2. Increase in FVIII levels after transduction with the simian immuno-deficiency virus (SIV) lentiviral vector. The induced pluripotent stem cells (iPSCs) were transduced with SIV vector expressing human B-domain deleted coagulation factor VIII (hBDD-FVIII) under the control of a CAG promoter (SIV-CAG-hFVIII) at an MOI of 30. (a) Schematic of the SIV vectors used in our experiments. (B) FVIII activities in the supernatants derived from cloned iPSCs (#4, #15, and #23) transduced with SIV-CAG-hFVIII were measured using a one-stage clotting time assay. Values are presented as means ±SD (*n* = 4 for each experiment). (c, d) iPSC clones expressing hFVIII were subcu-taneously transplanted into nude mice. (c) Teratoma weight at 4 weeks after subcutaneous transplantation of cloned MSC-iPSCs transduced with SIV-CAG-hFVIII. Values are presented as means ±SD (*n* = 3–5). (d) Plasma FVIII antigen levels in nude mice at the indicated times after subcutaneous trans-plantation of the iPSC clones. Values are means ±SD (*n* = 3–5).

completely avoided in their application. To reduce tu-mourigenicity and to improve the safety of iPSCs, the use of non-integrative vectors and changes of defined factors has been widely examined [6,23–25]. We also should differentiate iPSCs into the appropriate cells before transplantation, and plan to establish a more realistic cell therapy approach using immunocompetent FVIII-deficient mice.

One strategy to increase the safety of iPSCs for cell therapy would be to administer anucleated cells, such as red blood cells and platelets, differentiated from iPSCs. Integration of transgenes into genomic DNA during iPSC induction and lentiviral transduction might be negligible in the transplantation of anucleate cells. We have previously reported, along with other researchers, that expression of coagulation factor in red blood cells [26] and platelets [13,27] using lentiviral vectors has corrected the phenotype of mouse models of haemophilia. The use of blood cells to deliver coagulation factor is attractive as it avoids interference from circulating inhibitors. Recent reports have suggested the production of functional platelets from human iPSCs [28]; the transfusion of these blood cells expressing coagulation factor produced from iPSCs in vitro is possibly the most efficient and effective method for treating haemophiliacs.

In conclusion, we have proposed a new cell-based treatment for haemophilia involving iPSCs. Our proposed approach appears to be feasible, as transplantation of iPSCs resulted in increased and therapeutically appropriate FVIII plasma levels. Further investigations are needed to explore the risks of tumourigenicity from iPSC-derived cells, and to efficiently increase plasma levels of coagulation factor following cell therapy.

Acknowledgements

Disclosures

References

1 Mannucci PM, Tuddenham EG. The hemophilias–from royal genes to gene therapy. N Engl J Med 2001; 344: 1773–9.

2 Nathwani AC, Tuddenham EG, Rangarajan S et al. Adenovirus-associated virus vector-mediated gene transfer in hemophilia B. N Engl J Med 2011; 365: 2357–65.

3 Lillicrap D, VandenDriessche T, High K. Cellular and genetic therapies for haemophilia. Haemophilia 2006; 12(Suppl 3): 36–41.

4 Roth DA, Tawa NE Jr., O'Brien JM, Treco DA, Selden RF. Nonviral transfer of the gene encoding coagulation factor VIII in patients with severe hemophilia A. N Engl J Med 2001; 344: 1735–42.

5 Takahashi K, Yamanaka S. Induction of pluripotent stem cells from mouse embryonic and adult fibroblast cultures by defined factors. Cell 2006; 126: 663–76.

6 Okita K, Ichisaka T, Yamanaka S. Generation of germline-competent induced pluripotent stem cells. Nature 2007; 448: 313–7.

7 Kashiwakura Y, Ohmori T, Mimuro J et al. Intra-articular injection of mesenchymal stem cells expressing coagulation factor ameliorates hemophilic arthropathy in factor VIII-deficient mice. J Thromb Haemost 2012; 10: 1802–13.

8 Niibe K, Kawamura Y, Araki D et al. Purified mesenchymal stem cells are an efficient source for iPS cell induction. PLoS ONE 2011; 6: e17610.

9 Oda Y, Yoshimura Y, Ohnishi H et al. Induction of pluripotent stem cells from human third molar mesenchymal stromal cells. J Biol Chem 2010; 285: 29270–8.

10 Gonzalez F, Barragan Monasterio M, Tiscornia G et al. Generation of mouse-induced pluripotent stem cells by transient expression of a single nonviral polycistronic vector. Proc Natl Acad Sci USA 2009; 106: 8918–22.

11 Ogata K, Mimuro J, Kikuchi J et al. Expression of human coagulation factor VIII in adipocytes transduced with the simian immunodeficiency virus agmTYO1-based vector for hemophilia A gene therapy. Gene Ther 2004; 11: 253–9.

12 Nakajima T, Nakamaru K, Ido E, Terao K, Hayami M, Hasegawa M. Development of novel simian immunodeficiency virus vectors carrying a dual gene expression system. Hum Gene Ther 2000; 11: 1863–74.

13 Ohmori T, Mimuro J, Takano K et al. Efficient expression of a transgene in platelets using simian immunodeficiency virus-based vector harboring glycoprotein Ibalpha promoter: in vivo model for platelet-targeting gene therapy. FASEB J 2006; 20: 1522–4.

14 Kuzmenkin A, Liang H, Xu G et al. Functional characterization of cardiomyocytes derived from murine induced pluripotent stem cells in vitro. FASEB J 2009; 23: 4168–80.

15 Narazaki G, Uosaki H, Teranishi M et al. Directed and systematic differentiation of cardiovascular cells from mouse induced pluripotent stem cells. Circulation 2008; 118: 498–506.

16 Schenke-Layland K, Rhodes KE, Angelis E et al. Reprogrammed mouse fibroblasts differentiate into cells of the cardiovascular and hematopoietic lineages. Stem Cells 2008; 26: 1537–46.

17 Hanna J, Wernig M, Markoulaki S et al. Treatment of sickle cell anemia mouse model with iPS cells generated from autologous skin. Science 2007; 318: 1920–3.

18 Wernig M, Zhao JP, Pruszak J et al. Neurons derived from reprogrammed fibroblasts functionally integrate into the fetal brain and improve symptoms of rats with Parkinson's disease. Proc Natl Acad Sci USA 2008; 105: 5856–61.

19 Cantz T, Bleidissel M, Stehling M, Scholer HR. In vitro differentiation of reprogrammed murine somatic cells into hepatic precursor cells. Biol Chem 2008; 389: 889–96.

20 Kasuda S, Tatsumi K, Sakurai Y et al. Expression of coagulation factors from murine induced pluripotent stem cell-derived liver cells. Blood Coagul Fibrinolysis 2011; 22: 271–9.

21 Xu D, Alipio Z, Fink LM et al. Phenotypic correction of murine hemophilia A using an iPS cell-based therapy. Proc Natl Acad Sci USA 2009; 106: 808–13.

22 Alipio Z, Adcock DM, Waner M et al. Sustained factor VIII production in hemophiliac mice 1 year after engraftment with induced pluripotent stem cell-derived factor VIII producing endothelial cells. Blood Coagul Fibrinol 2010; 21: 502–4.

23 Kaji K, Norrby K, Paca A, Mileikovsky M, Mohseni P, Woltjen K. Virus-free induction of pluripotency and subsequent excision of reprogramming factors. Nature 2009; 458: 771–5.

24 Zhou H, Wu S, Joo JY *et al.* Generation of induced pluripotent stem cells using recombinant proteins. *Cell Stem Cell* 2009; 4: 381–4.

25 Fusaki N, Ban H, Nishiyama A, Saeki K, Hasegawa M. Efficient induction of transgene-free human pluripotent stem cells using a vector based on Sendai virus, an RNA virus that does not integrate into the host genome. *Proc Jpn Acad Ser B Phys Biol Sci* 2009; 85: 348–62.

26 Chang AH, Stephan MT, Sadelain M. Stem cell-derived erythroid cells mediate long-term systemic protein delivery. *Nat Biotechnol* 2006; 24: 1017–21.

27 Shi Q, Wilcox DA, Fahs SA *et al.* Lentivirus-mediated platelet-derived factor VIII gene therapy in murine haemophilia A. *J Thromb Haemost* 2007; 5: 352–61.

28 Takayama N, Nishimura S, Nakamura S *et al.* Transient activation of c-MYC expression is critical for efficient platelet generation from human induced pluripotent stem cells. *J Exp Med* 2010; 207: 2817–30.
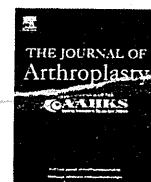
Changes in Blood Coagulation–Fibrinolysis Markers By Pneumatic Tourniquet During Total Knee Joint Arthroplasty With Venous Thromboembolism

Hideaki Watanabe, MD [a], Ichiro Kikkawa, MD [a], Seiji Madoiwa, MD [b], Hitoshi Sekiya, MD [a], Shinya Hayasaka, MD [c], Yoichi Sakata, MD [b]

[a] Department of Orthopedic Surgery, Jichi Medical University, Tochigi, Japan
[b] Research Division of Cell and Molecular Medicine, Center for Molecular Medicine, Jichi Medical University, Tochigi, Japan
[c] Department of Health Science, Daito Bunka University, Higashimatsuyama, Japan

ARTICLE INFO

ABSTRACT

This study investigated changes in blood coagulation–fibrinolysis markers during total knee arthroplasty (TKA). Preoperative 16-row multidetector row computed tomography (MDCT) revealed no asymptomatic venous thromboembolism (VTE) in the 42 patients recruited. Using MDCT postoperatively, patients were divided into thrombus (asymptomatic VTE, 19 patients) and no-thrombus (23 patients) groups. Blood taken at intervals before and after pneumatic tourniquet release revealed increased plasminogen activator inhibitor type-1 (PAI-1) at 30 s for both groups and at 90 s (both $P = 0.01$) in the thrombus group. D-dimer levels were highest at 30 and 90 s for both groups ($P = 0.01$). PAI-1 and D-dimer levels were strongly correlated at both time points in the thrombus group. Inactivating fibrinolysis due to PAI-1 may lead to asymptomatic VTE after TKA.

© 2014 Elsevier Inc. All rights reserved.

In orthopedic surgery, it is extremely important to prevent the development of postoperative venous thromboembolism (VTE), particularly symptomatic, fatal pulmonary embolism (PE), after total knee arthroplasty (TKA) [1]. Antithrombotic therapies using agents such as unfractionated or low-molecular-weight heparin have been administered to patients after surgery. Despite the implementation of aggressive antithrombotic protocols, however, the incidence of fatal PE remains at 0.15% [2] and that of symptomatic PE remains at 0.41% [3], with no changes in mortality rates since the 1990s [4]. Furthermore, in a cohort in Korea, the presence of asymptomatic VTE was 35.7% after TKA, as determined using multidetector row computed tomography (MDCT) [5]. Although it is thought that prophylactic antithrombotic treatments are necessary to prevent postoperative fatal and symptomatic PE, previous reports have found no difference in the incidence of these two entities or of asymptomatic VTE, regardless of whether prophylactic antithrombotic therapy was given [2–7]. In addition, reports indicate that the infection rate in prophylactically treated patients is increased owing to hematoma caused by hemorrhage [8–10] and coagulation abnormalities [11] associated with the therapy

early after surgery. It is important for orthopedic surgeons to avoid these complications because such infections can last a lifetime. Even if patients achieve remission, they are prone to infection relapse. The routine administration of prophylactic antithrombotic treatment is not recommended in East Asia [12]. Based on these observations, to reduce postoperative infections associated with the overuse of antithrombotic treatment in low-risk patients, we have considered it clinically important to be able to detect early asymptomatic VTE that may cause fatal or symptomatic PE after surgery in patients who are not administered prophylactic antithrombotic treatments. Also, we start antithrombotic therapy only in those patients who need it [6,13]. There are currently no blood coagulation–fibrinolysis markers available for early detection of postoperative asymptomatic VTE following TKA.

Since 2005, some studies have indicated that VTE is affected by the use of the pneumatic tourniquet, causing particular postoperative changes in coagulation–fibrinolysis pathways [14–17]. Therefore, we hypothesized that detecting changes in blood coagulation–fibrinolysis markers in patients with asymptomatic VTE immediately after the pneumatic tourniquet is released might be used to indicate whether patients require antithrombotic therapy. This information could help prevent postoperative bleeding after administering antithrombotics to patients who are at low risk of developing VTE. The purpose of this study was to investigate the changes of blood coagulation–fibrinolysis markers in asymptomatic VTE immediately after release of the pneumatic tourniquet during surgery.

Materials and Methods

Patients

The study protocol was approved by the Ethics Review Board of our university. This prospective, single-center study enrolled patients who underwent TKA at our institution between April 2007 and March 2009 and gave consent to participate in the study. As exclusion criteria, patients with a past history of symptomatic VTE, cerebral hemorrhage, cerebral infarction, cardiac infarction, or drug allergy to a contrast medium were excluded from the study. In addition, patients with liver disease, renal disease, and/or congenital clotting factor deficiencies and those undergoing antithrombotic therapy or hemodialysis were excluded from the study. Patients with asymptomatic VTE by preoperative MDCT were also excluded.

We enrolled 42 patients who underwent TKA for osteoarthritis (30 knees) or rheumatoid arthritis (12 knees). The cohort comprised 1 male and 41 female patients, with a mean age of 71 years (range 49–84 years). TKA was performed under general anesthesia in all patients, and a pneumatic tourniquet was used. Its pressure was raised before surgery while the leg was exsanguinated and lowered about 90 min later. The tourniquet was used only one time. The patients wore an elastic stocking on the unaffected leg during surgery. Later, they wore them on both affected and unaffected legs and used an intermittent pneumatic compression device until walking training was initiated, in accordance with the Japanese Guidelines for Prevention of Venous Thromboembolism [18]. No postoperative prophylactic antithrombotic therapy was administered. If the patients developed symptomatic VTE and/or if VTE was detected by MDCT, aggressive antithrombotic therapy was initiated.

MDCT

For diagnosis of VTE, 16-row MDCT was performed on the 4th day before surgery and then the 4th day after surgery. These time points mark the interval at which the incidences of PE and VTE are reported to be high [19]. The latter is the earliest point at which patients could comfortably undergo MDCT during the postoperative period.

The MDCT slice thicknesses were 2 mm in the thoracic region and 5 mm from the abdomen to the lower limbs. The window levels were 40–60 and 40–50, and the window widths were 400–500 and 200–400, respectively. A single radiologist (M.D.) evaluated the MDCT images in a blinded manner before and after the surgery. The incidence of postoperative new asymptomatic VTE was calculated.

Preoperative MDCT revealed no asymptomatic VTE in any of the 42 patients included in the study. The patients were classified postoperatively via MDCT into two groups. The thrombus group was defined as patients with a new asymptomatic VTE, and the no-thrombus group was defined as those without asymptomatic VTE.

Blood Coagulation–Fibrinolysis Markers

Blood samples were taken to measure the plasma levels of plasminogen activator inhibitor-1 (PAI-1), soluble fibrin monomer complex (SFMC), D-dimer, and cross-linked fibrin degradation products by leukocyte elastase (e-XDP) immediately before and after release of the pneumatic tourniquet and then at 30, 90, and 180 s after release of the pneumatic tourniquet (Fig. 1). Citrated

plasma samples were stored at −80 °C until analysis. The plasma PAI-1 levels were measured by a latex photometric immunoassay (Mitsubishi Chemical Medience Corporation, Tokyo, Japan) using the polyclonal antibody F(ab') fragment [20]. Plasma SFMC, D-dimer, and e-XDP levels were measured by latex immunoagglutination assays (Mitsubishi Chemical Medience Corporation) using the monoclonal antibodies IF-43 and JIF-23, respectively [21,22]. The plasma e-XDP levels were measured by a latex immunoagglutination assay (Mitsubishi Chemical Medience Corporation) using the monoclonal antibody IF-123 [23].

Statistical Analysis

Statistical analyses were performed using SPSS for Windows version 11.0 software (SPSS, Chicago, IL, USA). PAI-1, SFMC, D-dimer, and e-XDP levels were analyzed by the Shapiro–Wilk test if they did not fit a normal distribution. The PAI-1, SFMC, D-dimer, and e-XDP levels were compared between the thrombus and no-thrombus groups before release using the Mann–Whitney U-test. The PAI-1, SFMC, D-dimer and e-XDP levels were compared between immediately, at 30, 90, 180 s after release, respectively, and immediately before release using the Friedman test. If a significant difference was noted, the data were compared using the Wilcoxon signed rank test and corrected using Bonferroni's inequality. Spearman's rank correlation was used to determine whether blood coagulation–fibrinolysis markers that differed significantly were affected by each other. The gender and disorder distributions were compared between the thrombus and no-thrombus groups using Fisher's exact test. Age, volume of intraoperative hemorrhage, and operation time were compared using an unpaired t-test. The level of statistical significance was set at $P < 0.05$ for all tests.

Results

No patients developed symptomatic VTE during or after TKA in this study. Postoperative MDCT revealed asymptomatic VTE in 19 (45.2%) patients (thrombus group) and no VTE in 23 patients (54.7%) (no-thrombus group). Aggressive antithrombotic therapy was initiated in the 19 patients in whom new asymptomatic VTE was detected following postoperative MDCT (Table).

Changes in Operative Blood Coagulation–Fibrinolysis Markers Before Release of the Pneumatic Tourniquet

There were no significant differences in the preoperative PAI-1, SFMC, D-dimer, or e-XDP levels between the thrombus and no-thrombus groups ($P = 0.23$, $P = 0.23$, $P = 0.39$, and $P = 0.89$, respectively) (Fig. 2).

Operative Blood Coagulation–Fibrinolysis Markers After Release of the Pneumatic Tourniquet

The PAI-1 level showed the most significant increases at 30 s (median 27.3 ng/ml, $P = 0.01$) and 90 s (median 28.5 ng/ml, $P = 0.01$) after release of the pneumatic tourniquet in the thrombus groups and at 30 s (median 38.7 ng/ml, $P = 0.01$) after release in the no-thrombus group (Fig. 2).

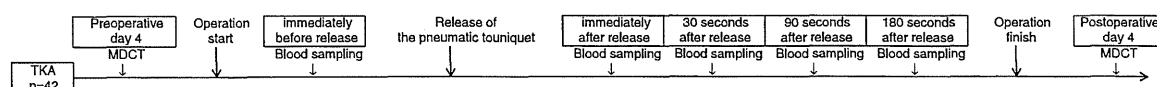| TKA n=42	Preoperative day 4 MDCT ↓	Operation start ↓	immediately before release Blood sampling ↓	Release of the pneumatic tourniquet ↓	immediately after release Blood sampling ↓	30 seconds after release Blood sampling ↓	90 seconds after release Blood sampling ↓	180 seconds after release Blood sampling ↓	Operation finish ↓	Postoperative day 4 MDCT ↓

Fig. 1. Study protocol.

Table
Study Demographics.

		Thrombus Group (n = 19)	No-Thrombus Group (n = 23)	P	95% Confidence Interval
Gender	Male:Female	0:19	1:22	0.55[a]	
Ages	Years	72 (60–82)	71 (49–84)	0.76[b]	−5 to 6
Disorder distribution	Osteoarthritis:Rheumatoid arthritis	13:6	17:6	0.48[a]	
Volume of intraoperative hemorrhage	ml	46 (0–120)	32 (0–260)	0.43[b]	−22 to 49
Operation time	min	155 (122–199)	148 (106–186)	0.31[b]	−7 to 21

[a] Fisher's exact test.
[b] Unpaired t-test.

The D-dimer level showed the most significant increases at 30 s (median 0.84 µg/ml, $P = 0.01$) and 90 s (median, 0.86 µg/ml, $P = 0.01$) after tourniquet release in the thrombus groups and at 30 s (median 0.73 µg/ml, $P = 0.01$) and 90 s (median 0.7 µg/ml, $P = 0.01$) after tourniquet release in the no-thrombus group (Fig. 2).

The SFMC and e-XDP levels did not differ significantly among the various time points before and after tourniquet release in the thrombus and no-thrombus groups (Fig. 2).

Spearman's rank correlation showed that the PAI-1 levels were strongly correlated with the D-dimer levels at 30 s ($\gamma = 0.57$, $P = 0.01$) and 90 s ($\gamma = 0.6$, $P = 0.01$) after tourniquet release in the thrombus group and were not correlated with the D-dimer levels at 30 s ($P = 1.00$) and 90 s ($P = 1.00$) after tourniquet release in the no-thrombus group (Fig. 3).

There was no significant difference in gender, age, volume of intraoperative hemorrhage, or operation time between the thrombus and no-thrombus groups (Table 1).
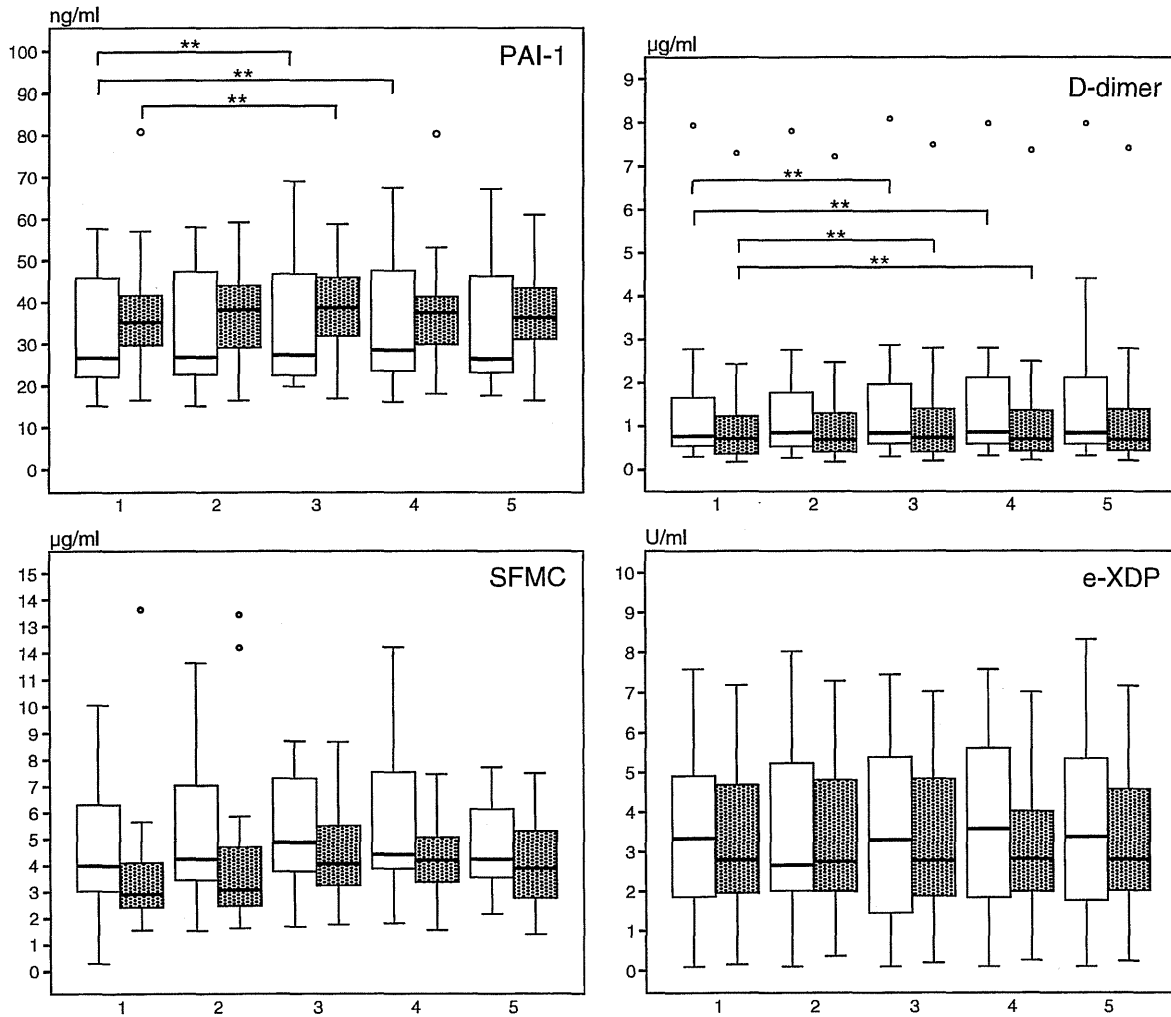
Fig. 2. Changes in the PAI-1 and SFMC, D-dimer, e-XDP levels before and after release of the pneumatic tourniquet. On the x-axis, the numbers correspond to the following: 1: immediately before release of the pneumatic tourniquet; 2: during; 3: at 30 s; 4: at 90 s; 5: at 180 s after release of the pneumatic tourniquet. White boxes, thrombus group; dot boxes, no-thrombus group. °Outlier. **$P < 0.05$ versus the preoperative level in the thrombus and the no-thrombus group by the Wilcoxon signed-rank test with correction by Bonferroni's inequality. PAI-1, plasminogen activator inhibitor-1; SFMC, soluble fibrin monomer complex; e-XDP, cross-linked fibrin degradation products by leukocyte elastase.
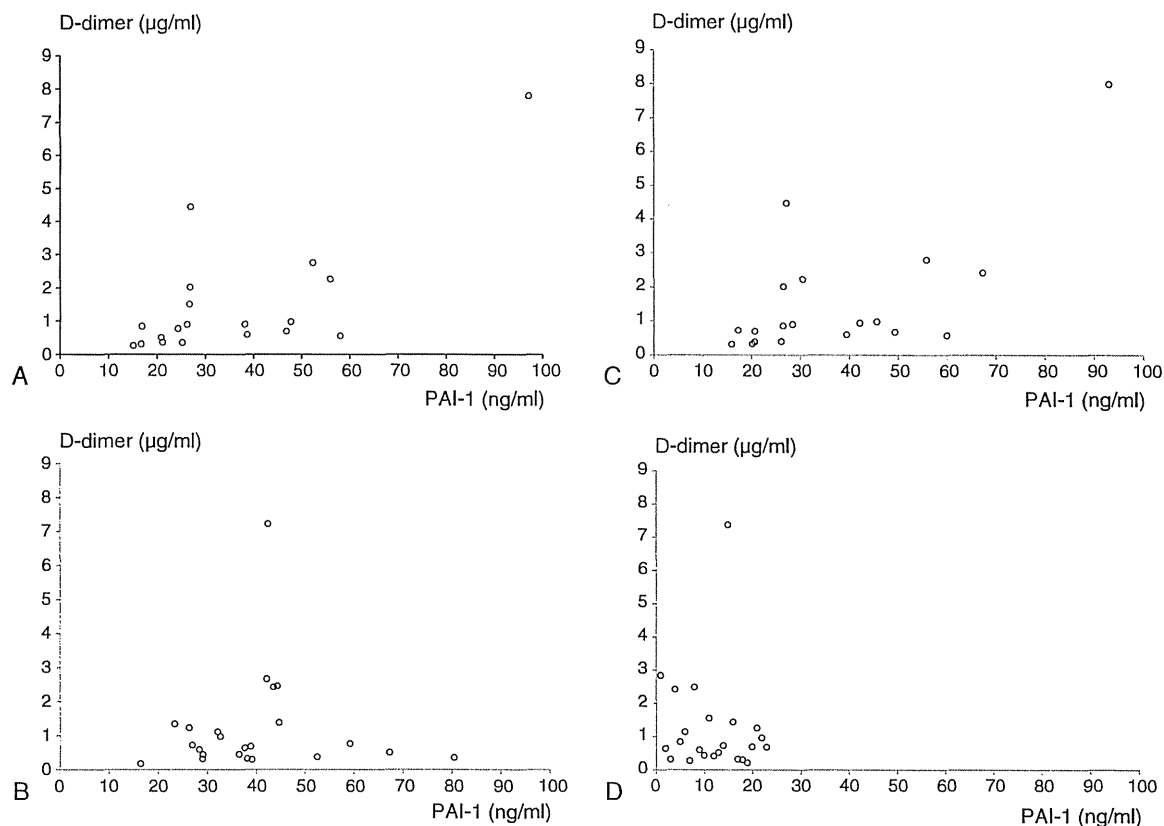
Fig. 3. Correlation between the PAI-1 and D-dimer levels at different time points. (A) At 30 s after release of the pneumatic tourniquet in the thrombus group ($P = 0.01$. $\gamma = 0.57$). (B) At 30 s after release of the pneumatic tourniquet in the no-thrombus group ($P = 1.00$). (C) At 90 s after release of the pneumatic tourniquet in the thrombus group ($P = 0.01$. $\gamma = 0.6$). (D) At 90 s after release of the pneumatic tourniquet in the no-thrombus group ($P = 1.00$). PAI-1, plasminogen activator inhibitor-1.

Discussion

Coagulation–fibrinolysis markers that may be predictive of postoperative asymptomatic DVT and VTE after TKA have been identified. Bounameaux et al [24] performed venography and D-dimer measurements on day 3 after TKA. They found that the D-dimer level was significantly elevated in patients with asymptomatic DVT and that the sensitivity and specificity were 58.8% and 73.5%, respectively, at a cutoff level of 3000 μg/ml. In 2000, Rever et al [25] performed venography after TKA and reported that the SFMC level was significantly elevated in patients with asymptomatic DVT on postoperative days 3 and 6. In 2012, Watanabe et al [26] performed MDCT after TKA and reported that the e-XDP level on postoperative day 1 and the D-dimer level on postoperative day 4 were significantly elevated in patients with asymptomatic VTE. They also noted that the sensitivity and specificity were 75% and 75%, respectively, for e-XDP levels and 59% and 63%, respectively, for D-dimer levels, with cutoff levels of 8.2 U/ml and 7.5 μg/ml, respectively.

Despite this work, there have been no reports of blood coagulation–fibrinolysis markers for predicting postoperative asymptomatic VTE in patients undergoing TKA. In the present study, the PAI-1 level at 90 s after release of the pneumatic tourniquet was significantly higher in the thrombus group than in the no-thrombus group. Furthermore, Spearman's rank correlation showed that PAI-1 was strongly correlated with D-dimer at 90 s ($\gamma = 0.6$, $P = 0.01$) after release in thrombus group and was not correlated with D-dimer at 90 s ($P = 1.00$) after release in the no-thrombus group. As there were no significant differences in gender, age, disorder distribution, volume of intraoperative hemorrhage, or operation time between the thrombus and no-thrombus groups, we can surmise that the PAI-1 level at 90 s after release of the

pneumatic tourniquet may be associated with asymptomatic VTE after TKA and is a dependent marker for D-dimer. D-dimer is produced by fibrin and the presence of a thrombus. An elevation in the D-dimer level indicates fibrinolysis of the thrombus. PAI-1 inactivates fibrinolysis by acting on the plasmin in the plasminogen activator–plasmin system. Therefore, we believe that increased inactivation of fibrinolysis leads to the development of asymptomatic VTE after TKA. A recent study has also demonstrated an association between PAI-1 levels and VTE after total hip arthroplasty [27]. If PAI-1 causes asymptomatic VTE and subsequent symptomatic, fatal PE, inactivation of PAI-1 may prevent the development of symptomatic, fatal PE. This study is a single-center study. If the results of future multicenter studies are similar, it may be stated that PAI-1 is likely to cause asymptomatic VTE and, subsequently, symptomatic, fatal PE.

The D-dimer levels at 30 and 90 s and PAI-1 levels at 30 s after release of the pneumatic tourniquet were significantly elevated in both groups compared with the values before tourniquet release. Katsumata et al [14] and Nishiguchi et al [15] measured changes in coagulation–fibrinolysis markers between patients with and without the pneumatic tourniquet after TKA. They identified significantly higher D-dimer levels immediately after surgery and on the first day with the pneumatic tourniquet. In a similar study, Reikeras et al [17] also found elevated D-dimer levels immediately after release of the pneumatic tourniquet. From these clinical studies and our study, we consider that the use of the pneumatic tourniquet during TKA affects the concentrations of blood coagulation–fibrinolysis markers and may cause thrombus formation. Thus, the pneumatic tourniquet should be used at little as possible during TKA.

The PAI-1 level was strongly correlated with the D-dimer level at 30 s ($R = 0.57$, $P = 0.01$) after release in thrombus group and was

not correlated with the D-dimer level at 30 s ($P = 1.00$) after release in no-thrombus groups. The PAI-1-like products that are not associated with fibrinolysis may be in the bone marrow and may be released into the bloodstream at an early time point after release of the pneumatic tourniquet.

One limitation of our study is that we do not know whether early detection of asymptomatic VTE prevents symptomatic, fatal PE. Therefore, we have continued to follow these patients in daily clinics after completion of this study. So far, none of the patients has suffered from symptomatic, fatal PE. Another limitation of our study is that MDCT was performed 4 days preoperatively and postoperatively, and the results therefore reflect the state of asymptomatic VTE at these time points. This is because the incidence of PE after TKA was reported to be high at postoperative days 3 or 4 [16]. Furthermore, day 4 was the earliest point during the postoperative period at which the patients had less pain and could comfortably undergo MDCT. However, because MDCT was not performed between the day of surgery and postoperative day 3, it can be assumed that not all asymptomatic VTEs were detected during the perisurgical period. Thus, the incidence of postsurgical asymptomatic VTE may be underestimated, and larger studies are required to verify the changes in coagulation–fibrinolysis markers in patients with asymptomatic VTE during surgery.

In summary, we investigated changes in blood coagulation–fibrinolysis markers during TKA in thrombus and no-thrombus groups using MDCT. PAI-1 levels were highest at 30 s in both groups and at 90 s in the thrombus group. D-dimer levels were highest at 30 and 90 s in both groups. PAI-1 and D-dimer levels were strongly correlated at both time points in the thrombus group, whereas they were not correlated in the no-thrombus group. Inactivating fibrinolysis due to PAI-1 may lead to the development of asymptomatic VTE and, subsequently, to symptomatic, fatal PE after TKA. Inactivation of PAI-1 may prevent the development of symptomatic, fatal PE after TKA.

Acknowledgments

References

1. Berend KR, Lombardi Jr AV. Multimodal venous thromboembolic disease prevention for patients undergoing primary or revision total joint arthroplasty: the role of aspirin. Am J Orthop 2006;35:24.
2. Howie C, Hughes H, Watts AC. Venous thromboembolism associated with hip and knee replacement over a ten-year period: a population study. J Bone Joint Surg Br 2005;87:1675.
3. Soohoo NF, Zingmond DS, Lieberman JR, et al. Primary total knee arthroplasty in California 1991 to 2001: does hospital volume affect outcomes? J Arthroplasty 2006;21:199.
4. Geerts WH, Heit JA, Clagett GP, et al. Prevention of venous thromboembolism. Chest 2001;119:132S.
5. Park KH, Cheon SH, Lee JH, et al. Incidence of venous thromboembolism using 64 channel multidetector row computed tomography indirect venography and anticoagulation therapy after total knee arthroplasty in Korea. Knee Surg Relat Res 2012;24:19.
6. Watanabe H, Sekiya H, Kariya Y, et al. The incidence of venous thromboembolism before and after total knee arthroplasty using 16-row multidetector computed tomography. J Arthroplasty 2011;26:1488.
7. Sharrock NE, Gonzalez Della Valle A, Go G, et al. Potent anticoagulants are associated with a higher all-cause mortality rate after hip and knee arthroplasty. Clin Orthop Relat Res 2008;466:714.
8. Saleh K, Olson M, Resig S, et al. Predictors of wound infection in hip and knee joint replacement: results from a 20 year surveillance program. J Orthop Res 2002;20:506.
9. Parvizi J, Ghanem E, Joshi A, et al. Does "excessive" anticoagulation predispose to periprosthetic infection? J Arthroplasty 2007;22:24.
10. Burnett RS, Clohisy JC, Wright RW, et al. Failure of the American College of Chest Physicians-1A protocol for lovenox in clinical outcomes for thromboembolic prophylaxis. J Arthroplasty 2007;22:317.
11. Saxena A, Baratz M, Austin MS, et al. Periprosthetic joint infection can cause abnormal systemic coagulation. J Arthroplasty 2011;26:50.
12. Cho KY, Kim KI, Khurana S, et al. Is routine chemoprophylaxis necessary for prevention of venous thromboembolism following knee arthroplasty in a low incidence population? Arch Orthop Trauma Surg 2013;133:551.
13. Abunasser J, Tejada JP, Foley RJ. The diagnosis and management of pulmonary embolism. Conn Med 2012;76:5.
14. Katsumata S, Nagashima M, Kato K, et al. Changes in coagulation–fibrinolysis marker and neutrophil elastase following the use of tourniquet during total knee arthroplasty and the influence of neutrophil elastase on thromboembolism. Acta Anaesthesiol Scand 2005;49:510.
15. Nishiguchi M, Takamura N, Abe Y, et al. Pilot study on the use of tourniquet: a risk factor for pulmonary thromboembolism after total knee arthroplasty? Thromb Res 2005;115:271.
16. Kageyama K, Nakajima Y, Shibasaki M, et al. Increased platelet, leukocyte, and endothelial cell activity are associated with increased coagulability in patients after total knee arthroplasty. J Thromb Haemost 2007;5:738.
17. Reikeras O, Clementsen T. Time course of the thrombosis and fibrinolysis in total knee arthroplasty with tourniquet application. Local versus systemic activations. J Thromb Thrombolysis 2009;28:425.
18. Editorial Committee on Japanese guideline for prevention of venous thromboembolism: digest. 2nd ed. Medical Front International Limited, Tokyo, 2004; p. 15–6.
19. Warwick D, Friedman RJ, Agnelli G, et al. Insufficient duration of venous thromboembolism prophylaxis after total hip or knee replacement when compared with the time course of thromboembolic events: findings from the Global Orthopaedic Registry. J Bone Joint Surg Br 2007;89:799.
20. Ono T, Sogabe M, Ogura M, et al. Automated latex photometric immunoassay for total plasminogen activator inhibitor-1 in plasma. Clin Chem 2003;49:987.
21. Soe G, Kohno I, Inuzuka K, et al. A monoclonal antibody that recognizes a neo-antigen exposed in the E domain of fibrin monomer complexed with fibrinogen or its derivatives: its application to the measurement of soluble fibrin in plasma. Blood 1996;88:2109.
22. Matsuda M, Terukina S, Yamazumi K, Maekawa H, Soe G. A monoclonal antibody that recognizes the NH2-terminal conformation of fragment D. p. 43–8. In: Fibrinogen 4, current basic and clinical aspects: proceedings of the International Fibrinogen Workshop, Kyoto, Japan, 27–28 August 1989. Amsterdam: Excerpta Medica; 1990: 43–8.
23. Kohno I, Inuzuka K, Itoh Y, et al. A monoclonal antibody specific to the granulocyte-derived elastase-fragment D species of human fibrinogen and fibrin: its application to the measurement of granulocyte-derived elastase digests in plasma. Blood 2000;95:1721.
24. Bounameaux H, Miron MJ, Blanchard J, et al. Measurement of plasma D-dimer is not useful in the prediction or diagnosis of postoperative deep vein thrombosis in patients undergoing total knee arthroplasty. Blood Coagul Fibrinolysis 1998;9:749.
25. Rever G, Blanchard J, Bounameaux H, et al. Inability of serial fibrin monomer measurements to predict or exclude deep venous thrombosis in asymptomatic patients undergoing total knee arthroplasty. Blood Coagul Fibrinolysis 2000;11:305.
26. Watanabe H, Madoiwa S, Sekiya S, et al. Predictive blood coagulation markers for early diagnosis of venous thromboembolism after total knee joint replacement. Thromb Res 2011;128:e137.
27. Yukizawa Y, Inaba Y, Watanabe S, et al. Association between venous thromboembolism and plasma levels of both soluble fibrin and plasminogen-activator inhibitor 1 in 170 patients undergoing total hip arthroplasty. Acta Orthop 2012;83:14.

ORIGINAL BASIC RESEARCH   Open Access

Paxillin is an intrinsic negative regulator of platelet activation in mice

Asuka Sakata[1,2], Tsukasa Ohmori[1*], Satoshi Nishimura[1,3,4], Hidenori Suzuki[5], Seiji Madoiwa[1], Jun Mimuro[1], Kazuomi Kario[2] and Yoichi Sakata[1]

Abstract

Background: Paxillin is a LIM domain protein localized at integrin-mediated focal adhesions. Although paxillin is thought to modulate the functions of integrins, little is known about the contribution of paxillin to signaling pathways in platelets. Here, we studied the role of paxillin in platelet activation in vitro and in vivo.

Methods and results: We generated paxillin knockdown (Pxn-KD) platelets in mice by transplanting bone marrow cells transduced with a lentiviral vector carrying a short hairpin RNA sequence, and confirmed that paxillin expression was significantly reduced in platelets derived from the transduced cells. Pxn-KD platelets showed a slight increased in size and augmented integrin αIIbβ3 activation following stimulation of multiple receptors including glycoprotein VI and G protein-coupled receptors. Thromboxane A_2 biosynthesis and the release of α-granules and dense granules in response to agonist stimulation were also enhanced in Pxn-KD platelets. However, Pxn-KD did not increase tyrosine phosphorylation or intracellular calcium mobilization. Intravital imaging confirmed that Pxn-KD enhanced thrombus formation in vivo.

Conclusions: Our findings suggest that paxillin negatively regulates several common platelet signaling pathways, resulting in the activation of integrin αIIbβ3 and release reactions.

Keywords: Platelet, Glycoprotein, Platelet aggregation, Release reaction

Background

A breakdown of normal platelet function results in either unexpected bleeding or thrombotic events [1]. Platelets are inactive in the intact vasculature under physiological conditions. However, once the platelets encounter an injured region of the endothelium, they attach through an interaction between von Willebrand factor and the glycoprotein (GP) Ib/IX/V complex [2], and then collagen receptor GPVI triggers platelet activation. Activated platelets release several classes of agonists, including ADP and thromboxane (Tx) A_2, which promote further platelet activation [3]. These steps ultimately increase the affinity of integrin αIIbβ3 for its ligands and induce platelet aggregation [4]. The intracellular signaling that increases the affinity of integrins is known as inside-out signaling [4]. Multiple signal transduction pathways from various

receptors share common inside-out signaling cascades. For example, phosphoinositol hydrolysis, which leads to calcium mobilization and protein kinase C activation [5], and Rap1b activation are well-known signaling pathways that regulate integrin-mediated platelet functions [6].

To increase the affinity of integrin αIIbβ3, inside-out signaling pathways induce a drastic conformational change of the integrin [7]. Direct interactions between cytoskeletal proteins (e.g., talin and kindlin) and cytoplasmic β integrin are essential for inducing the conformational change of integrins [7]. Indeed, the loss of talin or kindlin in platelets dramatically reduces integrin αIIbβ3-mediated platelet aggregation, despite normal expression levels of the surface receptors [8,9]. Selective blockade of talin binding by a single amino acid substitution in β3 integrin also impairs integrin αIIbβ3-dependent platelet responses [10]. Although a number of integrin-associated proteins have been reported [11], the identities of proteins and their roles in regulating integrin signaling in platelets have not been fully characterized. It is also unknown whether

* Correspondence: tohmori@jichi.ac.jp
[1]Research Division of Cell and Molecular Medicine, Center for Molecular Medicine, Jichi Medical University School of Medicine, 3111-1 Yakushiji, Shimotsuke, Tochigi 329-0498, Japan
Full list of author information is available at the end of the article

additional molecules, other than talin and kindlin, are capable of regulating integrin signaling pathways.

Paxillin is a LIM domain protein that was originally identified as a substrate for oncogene *v-src* [12]. Paxillin contains two conserved structural domains, the N-terminus and C-terminus, which consist of four LIM domains [13,14]. Two other family members have also been identified, Hic-5 and leupaxin [13,14]. Paxillin is ubiquitously expressed alongside these variants [13,14], except in human platelets that predominantly express Hic-5 [15,16]. Conversely, mouse platelets express paxillin and leupaxin in addition to Hic-5 [17]. Considering the multiple interaction motifs located within its structure, paxillin appears to serve as a signaling platform for the recruitment of numerous regulatory proteins near integrins [13,14]. Paxillin directly interacts with the cytoplasmic domain of integrin α4 and α9, but not αIIb, and these interactions controls integrin-mediated cell migration and spreading [18,19].

Integrin αIIbβ3 in platelets is suitable for studies of integrin receptors because its ligand binding and signal transduction pathways are well characterized. Elucidating the intracellular proteins involved in the activation of integrin αIIbβ3 can provide a better understanding of the functions of integrins and might result in the discovery of new antithrombotic targets [20]. We previously reported that lentiviral vector-mediated short hairpin RNA (shRNA) expression in hematopoietic stem cells greatly reduces the expression of the target protein in platelets [21]. This method enables functional analyses of target proteins that modulate platelet activation in anucleate platelets [21]. In the present study, we used this method to investigate the roles of paxillin in platelet activation, and found that paxillin negatively regulates platelet signaling pathways including the activation of integrin αIIbβ3 and release reactions.

Materials and methods

Materials

All mouse cytokines were purchased from PeproTech (London, UK). The following antibodies and agonists were obtained from the specified suppliers: PAC-1 monoclonal antibody (mAb), anti-mouse P-selectin mAb (RB40.34), anti-paxillin mAb (clone 349), and anti-Hic-5 mAb (BD Biosciences, San Jose, CA); horseradish peroxidase-conjugated anti-green fluorescent protein (GFP) polyclonal antibody (Acris Antibodies, Himmelreich, Germany); phycoerythrin (PE)-Cy7-conjugated anti-mouse IgM (eBioscience, San Diego, CA); anti-talin mAb (clone 8D4); anti-phosphotyrosine mAb (clone 4G10), and BAPTA-AM (Millipore, Billerica MA); human fibrinogen and epinephrine (Sigma-Aldrich, St. Louis, MO); anti-vinculin mAb (V284) (Chemicon, Billerica, MA); anti-mouse GPVI mAb (Six.E10), anti-mouse GPIbα mAb (Xia.G5), and anti-mouse integrin αIIbβ3 mAb (Leo.D2 and clone JON/A) (Emfret Analytics, Eibelstadt, Germany); anti-α-actin mAb (D6F6), anti-FAK polyclonal antibody, and anti-Src mAb (32G6) (Cell Signaling Technology, Danvers, MA); anti-Rap1b polyclonal antibody and anti-protein kinase Cα mAb (M4) (Upstate Cell Signaling Solutions, Lake Placid, NY); allophycocyanin (APC)-conjugated anti-rat IgG polyclonal antibody (R& D Systems, Minneapolis, MN); convulxin (ALEXIS Biochemicals, Plymouth Meeting, PA); AYPGKF (Invitrogen, Carlsbad, CA); ADP (MC medical, Tokyo, Japan); U46619 (Cayman Chemical, Ann Arbor, MI).

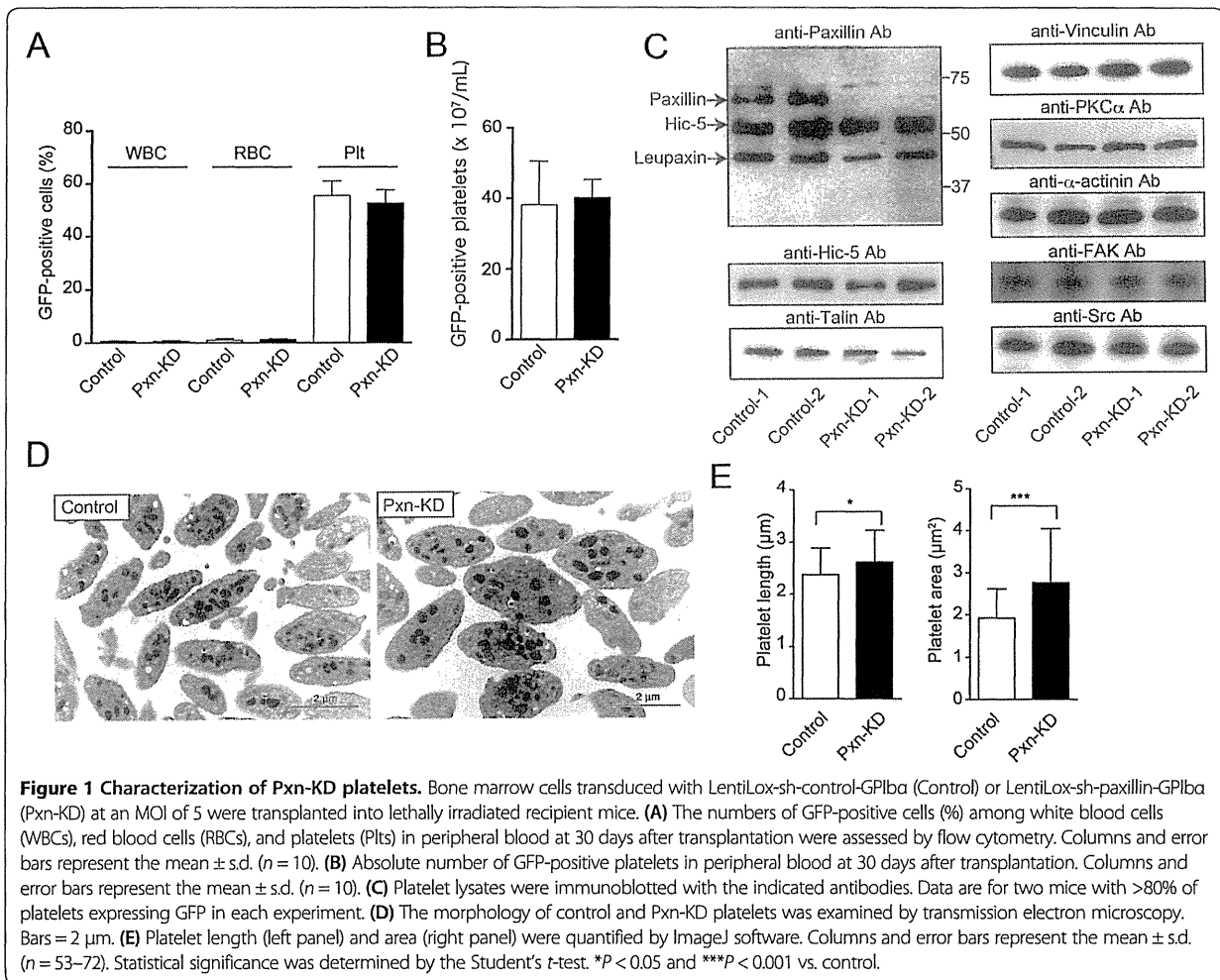### Lentiviral vector and virus production

A lentiviral vector plasmid for expression of shRNA sequences and GFP (LentiLox vector) was purchased from the American Type Culture Collection (Manassas, VA) [22]. To efficiently express GFP in platelets, the cytomegalovirus promoter of the LentiLox vectors was substituted with the platelet-specific GPIbα promoter (LentiLox-GPIbα) [21]. Putative shRNA sequences were designed using web-based software provided by Thermo Scientific Molecular Biology (http://www.thermoscientificbio.com/design-center/). Three shRNA sequences were synthesized for mouse paxillin and then cloned into a LentiLox vector plasmid (Additional files 1 and 2). Lentiviruses were produced as described previously [23].

Transplantation of mouse bone marrow cells

All animal procedures were approved by the Institutional Animal Care and Concern Committee of Jichi Medical University, and animal care was performed in accordance with the committee's guidelines. Mouse bone marrow cells (C57BL/6 J) were isolated and resuspended in StemPro®-34 SFM medium (Invitrogen) supplemented with 100 ng/mL each of stem cell factor, thrombopoietin, interleukin-6, and fms-like tyrosine kinase 3 ligand, and 200 ng/mL soluble interleukin-6 receptor. The lentiviral vector was added at 12–16 h after cell isolation (multiplicity of infection [MOI] = 5), and the cell culture was continued for 21–22 h. Each recipient mouse (8–12 weeks of age) was irradiated with a single lethal dose of 9.5 Gy and then intravenously injected with 2×10^6 lentivirus-transduced bone marrow cells. After transplantation, about 50% of platelets expressed GFP (Figure 1). Mice with 70% of their platelets exhibiting GFP positivity were used in experiments that could not distinguish GFP-positive platelets, *i.e.*, light transmission aggregometry, clot retraction, release concentration, calcium mobilization, and intravital microscopy.

Immunoblotting

Immunoblotting with the specific antibodies was performed as described previously [21]. To assess protein tyrosine phosphorylation, washed platelets were pretreated

Figure 1 Characterization of Pxn-KD platelets. Bone marrow cells transduced with LentiLox-sh-control-GPlbα (Control) or LentiLox-sh-paxillin-GPlbα (Pxn-KD) at an MOI of 5 were transplanted into lethally irradiated recipient mice. **(A)** The numbers of GFP-positive cells (%) among white blood cells (WBCs), red blood cells (RBCs), and platelets (Plts) in peripheral blood at 30 days after transplantation were assessed by flow cytometry. Columns and error bars represent the mean ± s.d. (n = 10). **(B)** Absolute number of GFP-positive platelets in peripheral blood at 30 days after transplantation. Columns and error bars represent the mean ± s.d. (n = 10). **(C)** Platelet lysates were immunoblotted with the indicated antibodies. Data are for two mice with >80% of platelets expressing GFP in each experiment. **(D)** The morphology of control and Pxn-KD platelets was examined by transmission electron microscopy. Bars = 2 μm. **(E)** Platelet length (left panel) and area (right panel) were quantified by ImageJ software. Columns and error bars represent the mean ± s.d. (n = 53–72). Statistical significance was determined by the Student's t-test. *P < 0.05 and ***P < 0.001 vs. control.

with 1 mmol/L EDTA, 5 U/mL apyrase, and 10 μmol/L SQ29548 to exclude the effects of aggregation, released ADP, and TxA₂.

Transmission electron microscopy

Mouse platelet pellets were fixed in 2% glutaraldehyde in 0.1 mol/L phosphate buffer (pH 7.4) for 60 min at 4°C. The samples were washed, post-fixed with 1% osmium tetroxide in 0.1 mol/L phosphate buffer for 60 min at 4°C, dehydrated with a graded ethanol series, and then embedded in Epon (TAAB Laboratories, Aldermaston, UK) as described previously [24]. Ultrathin sections were prepared, stained with uranyl acetate and lead citrate, and then examined under a JEM1010 transmission electron microscope (JEOL, Tokyo, Japan) at an accelerating voltage of 80 kV. The length and area of platelets were quantified using ImageJ Ver. 10.2 for Macintosh (NIH, Bethesda, MD).

Preparation of washed mouse platelets and flow cytometry

A blood sample (100–400 μL) was drawn from each mouse through the right jugular vein using a 30 G syringe containing 1/10 sodium citrate, and then diluted with 3 mL Hepes/Tyrode buffer (138 mmol/L NaCl, 3.3 mmol/L NaH₂PO₄, 2.9 mmol/L KCl, 1 mmol/L MgCl₂, 1 mg/mL glucose, and 20 mmol/L Hepes, pH 7.4). The diluted blood was centrifuged at 120 ×g for 8 min, and the platelets obtained from the platelet-rich fraction were washed and resuspended in Hepes/Tyrode buffer. Just prior to centrifugation, a 15% acid-citrate-dextrose A solution and 0.1 μmol/L prostaglandin I₂ were added to inhibit platelet activation. The final platelet suspensions were adjusted to 1 × 10⁷ platelets/mL and supplemented with 1 mmol/L CaCl₂. To assess the binding of JON/A, a monoclonal antibody (mAb) that recognizes activated mouse αIIbβ3 [25], to platelets, 30 μL of washed platelets was incubated with 4 μL of agonist solution, 4 μL of phycoerythrin (PE)-

conjugated JON/A and 1 μL of biotin-conjugated anti-mouse P-selectin mAb for 5 min, and then supplemented with 1 μL of allophycocyanin (APC)-conjugated strep-tavidin. After 15 min of incubation, JON/A binding and P-selectin expression were determined by flow cytometry using a FACSAria Cell Sorter (Becton Dickinson, Mountain View, CA). Antibody binding was quantified as the mean fluorescence intensity (MFI) of GFP-positive platelets.

Platelet aggregation

Washed platelets were prepared as described above. The final suspensions were adjusted to 2×10^8 platelets/mL and supplemented with 1 mmol/L $CaCl_2$ and 200 μg/mL fibrinogen. The aggregation response to agonist stimulation was measured based on light transmission measured using a PA-200 platelet aggregation analyzer (Kowa, Tokyo, Japan).

Measurement of platelet products

Washed platelets (2×10^8/mL) were stimulated with the indicated agonists for 15 min, and then the supernatants were recovered by centrifugation. The levels of platelet factor 4 (PF4) and serotonin in the supernatants were measured using a mouse PF4 enzyme-linked immunosorbent assay (ELISA) kit (R & D Systems) and an anti-serotonin ELISA kit (GenWay Biotech, San Diego, CA), respectively. The levels of TxB_2 in the supernatants were measured using an enzyme immunoassay (Cayman Chemical).

Platelet adhesion

Platelet adhesion to fibrinogen was assessed as described previously [21]. Briefly, eight-well dishes (Lab-Tek® Chamber Slide™) were coated with 400 μg/mL fibrinogen and then blocked with 1 mg/mL bovine serum albumin (BSA). Platelets were then added to the fibrinogen-coated dishes and incubated for 30 min at 37°C. Adherent platelets were fixed with 3% paraformaldehyde and then permeabilized with phosphate-buffered saline (PBS) containing 0.3% Triton X-100 and 5% donkey serum. After washing with PBS, the platelets were incubated with an anti-GFP polyclonal antibody (MBL, Aichi, Japan). Bound antibodies were detected by Alexa Fluor 488-conjugated anti-rabbit IgG. Actin filaments were detected by staining with 1 μg/mL rhodamine-conjugated phalloidin. Immuno-fluorescence staining was observed and photographed under a confocal microscope (FV1000; Olympus, Tokyo, Japan). The spread area of GFP-positive platelets was quantified using ImageJ software. Because Pxn-KD platelets were slightly larger than control platelets (Figure 1), the mean platelet size determined by BSA staining was subtracted from the total area on fibrinogen to calculate the actual increase in platelet spreading.

Clot retraction

Human platelet-poor plasma was mixed with the same volume of Hepes/Tyrode buffer containing washed mouse platelets (final concentration: 3×10^8 platelets/ml). Plasma coagulation was initiated by addition of 0.1 U/mL thrombin. The clots were photographed at various time points after thrombin addition. When indicated, 0.5 mmol/L manganese was added to exclude the role of inside-out signaling. The two-dimensional area of serum formation extruded by clot retraction was quantified using ImageJ software and expressed as the progression of clot retraction.

Calcium mobilization

Platelets were incubated with GFP-Certified™ FluoForte™ dye (Enzo Life Sciences, Farmingdale, NY). The fluorophore-loaded platelets (2×10^8/mL) were resuspended in Hepes-Tyrode buffer containing 1 mmol/L EDTA, 5 U/mL apyrase, and 10 μmol/L SQ29548 to exclude the effects of aggregation, extracellular calcium, released ADP, and TxA_2. After stimulation, the intracellular calcium concentration was determined by monitoring the fluorescence (excitation, 530 nm; emission, 570 nm) using a microplate spectrofluorometer (Gemini EM; Molecular Devices, Sunnyvale, CA).

Intravital microscopy and thrombus formation

Intravital microscopy was performed to analyze thrombus formation in vivo as reported previously [26]. Briefly, Texas Red-dextran (100 mg/kg body weight [BW], molecular weight: 70 kDa; Invitrogen), Hoechst 33342 (10 mg/kg BW; Invitrogen), Dylight 488-conjugated anti-CD42b antibody (200 μg/kg BW; Emfret), and hematoporphyrin (5 mg/kg BW; Sigma) were injected into anesthetized mice to produce reactive oxygen species (ROS) following laser irradiation. Blood cell dynamics were visualized during laser excitation (wavelengths 405, 488, and 561 nm; 1.5 mW total power at 100× objective lens). After laser irradiation, sequential images of the mesentery were obtained using a resonance scanning confocal microscope (Nikon A1R; Nikon, Tokyo, Japan). The areas of thrombus (shown by anti-CD42b antibody signals) before and after laser irradiation were calculated using NIS-Elements AR 3.2 (Nikon). When indicated, thrombus formation in the femoral artery was triggered by topical application of a filter paper tip saturated with 10% $FeCl_3$. After injection of Texas Red-dextran, Hoechst 33342, and Dylight 488-conjugated anti-CD42b antibody, thrombus formation was visualized and monitored by confocal microscopy using two photon microscopy (excitation wavelength 840 nm) by NikonA1R MP (Nikon).

Bleeding time

The distal tail tip (5 mm) of an anesthetized mouse was clipped, and the tail was immediately immersed in PBS

at 37°C. Tail bleeding times were defined as the time required for the bleeding to stop.

Results

Generation of paxillin knockdown (Pxn-KD) platelets

To address the function of paxillin in mouse platelets, we used a lentiviral vector carrying shRNA sequences and GFP [22]. We synthesized three shRNA sequences for mouse paxillin, and cloned them into a LentiLox vector plasmid (Additional files 1 and 2). We selected one sequence that significantly inhibited paxillin expression in embryonic fibroblasts after transduction (Pxn-1 sequence; Additional files 1 and 2). After transplantation of bone marrow cells transduced with either the control or Pxn-KD sequence, about 50% of the platelets expressed GFP, and the absolute numbers of GFP-positive platelets did not differ between experiments using control and Pxn-KD sequences (Figure 1A–B). Furthermore, there was no effect on the total number of platelets (control: 6.8 ± 1.72 × 10^8/mL; Pxn-KD: 7.7 ± 0.65 × 10^8/mL, $P = 0.18$). We compared the platelet aggregation response and release reaction in platelets from wild-type C57BL/6 J and control mice, and confirmed that platelet aggregation as well as the release reaction did not differ (data not shown). To confirm knockdown of paxillin in GFP-positive platelets, we selected mice in which more than 80% of platelets expressed GFP after transplantation. Immunoblotting of platelet lysates with an anti-paxillin mAb (clone 349) showed a marked reduction in paxillin expression following transplantation of bone marrow cells transduced with the Pxn-KD sequence (Figure 1C). This antibody also recognizes other members of the paxillin family, including Hic-5 and leupaxin [17]. However, Hic-5 and leupaxilin were not affected by expression of the Pxn-KD sequence (Figure 1C). Transmission electron microscopy of resting platelets revealed that the Pxn-KD platelets were slightly larger than control platelets (Figure 1D–E). This change was largely dependent on an increase of the cytoplasm volume, but not the granule volume (Additional file 3). Pxn-KD platelets showed marginally elevated expression levels of GPIb and integrin αIIbβ3, even though GPVI expression was normal (Additional file 4). These changes in Pxn-KD platelets were supposed to result from the increase in platelet size.

Augmentation of integrin αIIbβ3 activation in Pxn-KD platelets

We first focused on the role of paxillin in integrin αIIbβ3 activation that is critical for platelet aggregation. We performed flow cytometric analysis of integrin αIIbβ3 activation using an anti-JON/A mAb [25]. GFP-positive Pxn-KD platelets (Figure 2A, lower panel) showed significantly enhanced αIIbβ3 activation following stimulation compared with that of control platelets (Figure 2A, upper panel).

Enhanced JON/A binding of Pxn-KD platelets was observed following stimulation with the GPVI agonist convulxin and G protein-coupled receptor agonists including a protease-activated receptor 4 agonist (AYPGKF), ADP, and U46619 (Figure 2A–B). However, JON/A binding was not enhanced in unstimulated or epinephrine-stimulated platelets, suggesting that Pxn-KD alone does not induce activation of integrin αIIbβ3. We next used light transmission aggregometry to assess platelet aggregation in vitro. We found that platelet aggregation was significantly augmented in Pxn-KD platelets, and this effect was evident at low agonist concentrations that induce platelet aggregation (Figure 2C–D).

Enhanced release reactions and Tx biosynthesis in Pxn-KD platelets

We next assessed the release reactions in response to stimulation. To address the role of paxillin in α-granule secretion, P-selectin expression was determined in GFP-positive platelets by flow cytometry. As shown in Figure 3A–B, P-selectin expression in Pxn-KD platelets was significantly increased following stimulation with convulxin, AYPGKF, and U46619. In contrast, P-selectin expression was not increased by stimulation with ADP or epinephrine. We observed negligible increases in P-selectin expression of Pxn-KD platelets under the resting condition and after incubation with the fibronectin peptide Gly-Arg-Gly-Asp-Ser (GRGDS) (Figure 3B). To examine whether Pxn-KD platelets are already activated during circulation, we compared P-selectin expression in washed platelets and whole blood platelets before the preparation. An increase of P-selectin expression after washing the platelet preparation was observed in Pxn-KD platelets (30.0 ± 9.71 to 37.2 ± 5.72 in the control vs. 27.8 ± 2.56 to 44.8 ± 7.87, $P < 0.05$), suggesting that the susceptibility of Pxn-KD platelets caused marginal activation during washing. Although PF4 and serotonin content in resting platelets did not differ between control and Pxn-KD platelets (Additional file 3), the actual release of PF4 and serotonin into the supernatant in response to platelet activation was also enhanced in Pxn-KD platelets (Figure 3C–D). Of note, a marked increase in TxB_2 biosynthesis was observed in Pxn-KD platelets (Figure 3E). Pretreatment with the ADP scavenger apyrase and thromboxane A_2 receptor antagonist SQ29548 somewhat corrected the increase of JON/A binding in Pxn-KD platelets. This result suggests that the extent of the increase of integrin activation is partially dependent on the release reaction (Additional file 5). Collectively, these data suggest that paxillin negatively regulates platelet activation signaling pathways leading to integrin activation, release reactions, and Tx synthesis. It is possible that general pathway (s) involved in platelet activation were enhanced by Pxn-KD, because platelet activation was increased in
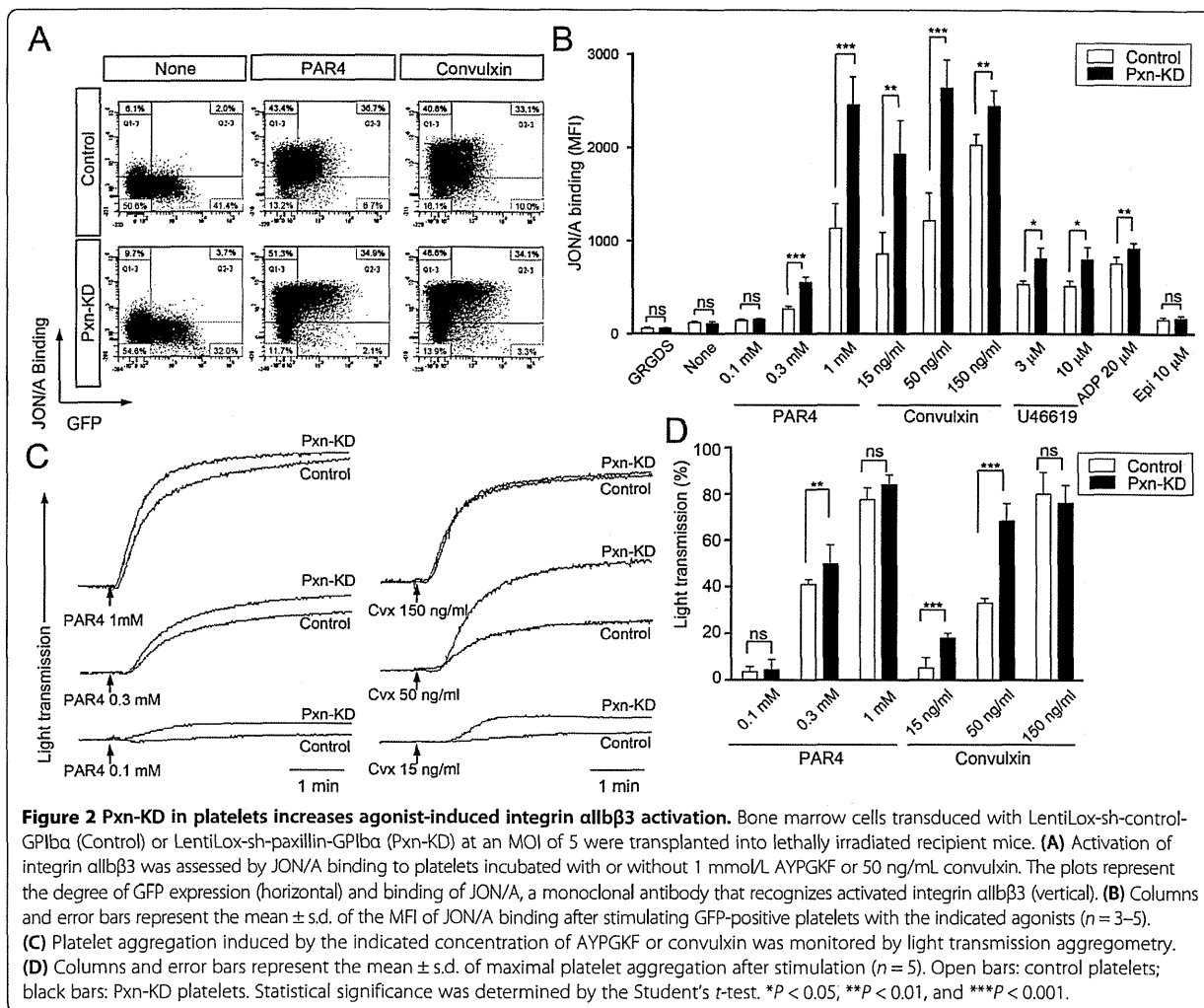
Figure 2 Pxn-KD in platelets increases agonist-induced integrin αIIbβ3 activation. Bone marrow cells transduced with LentiLox-sh-control-GPIbα (Control) or LentiLox-sh-paxillin-GPIbα (Pxn-KD) at an MOI of 5 were transplanted into lethally irradiated recipient mice. **(A)** Activation of integrin αIIbβ3 was assessed by JON/A binding to platelets incubated with or without 1 mmol/L AYPGKF or 50 ng/mL convulxin. The plots represent the degree of GFP expression (horizontal) and binding of JON/A, a monoclonal antibody that recognizes activated integrin αIIbβ3 (vertical). **(B)** Columns and error bars represent the mean ± s.d. of the MFI of JON/A binding after stimulating GFP-positive platelets with the indicated agonists (n = 3–5). **(C)** Platelet aggregation induced by the indicated concentration of AYPGKF or convulxin was monitored by light transmission aggregometry. **(D)** Columns and error bars represent the mean ± s.d. of maximal platelet aggregation after stimulation (n = 5). Open bars: control platelets; black bars: Pxn-KD platelets. Statistical significance was determined by the Student's t-test. *P < 0.05, **P < 0.01, and ***P < 0.001.

response to several classes of activators including GPVI and G protein-coupled receptors.

Assessment of outside-in signaling pathways in Pxn-KD platelets

To address the role of paxillin in outside-in signaling of integrin αIIbβ3, we assessed platelet spreading on fibrinogen and clot retraction. The cell area independent of integrin outside-in signaling (i.e., adherent to the BSA control) was slightly increased in Pxn-KD platelets compared with that in control platelets (data not shown), because the Pxn-KD platelets were marginally larger than control platelets (Figure 1). To quantify the increase in platelet spreading, the mean platelet size on BSA was subtracted from the total spreading area on fibrinogen. As shown in Figure 4A, the increase in platelet spreading on fibrinogen without or with convulxin stimulation was significantly greater for Pxn-KD platelets than that for control platelets (Figure 4A–B). In addition, clot retraction

induced by thrombin was significantly enhanced in Pxn-KD platelets compared with that in control platelets (Figure 4C–D). Acceleration of clot retraction in Pxn-KD platelets was also observed in the presence of manganese at 15 min (6.98 ± 0.130 vs. 7.56 ± 0.072, P < 0.05). These observations suggest that paxillin is an important regulator of integrin outside-in signaling via integrin αIIbβ3.

The role of paxillin in calcium mobilization in platelets

Because GPVI initiates signaling cascades by activation of non-receptor tyrosine kinases, we assessed tyrosine phosphorylation elicited by the GPVI signaling pathway. As a result, tyrosine phosphorylation events induced by convulxin were not affected by Pxn-KD (Figure 5A). The agonist-induced increase in intracellular calcium mobilization is an important common and proximal signaling event controlling platelet activation. Therefore, we next examined whether Pxn-KD enhanced intracellular calcium mobilization following stimulation. To exclude
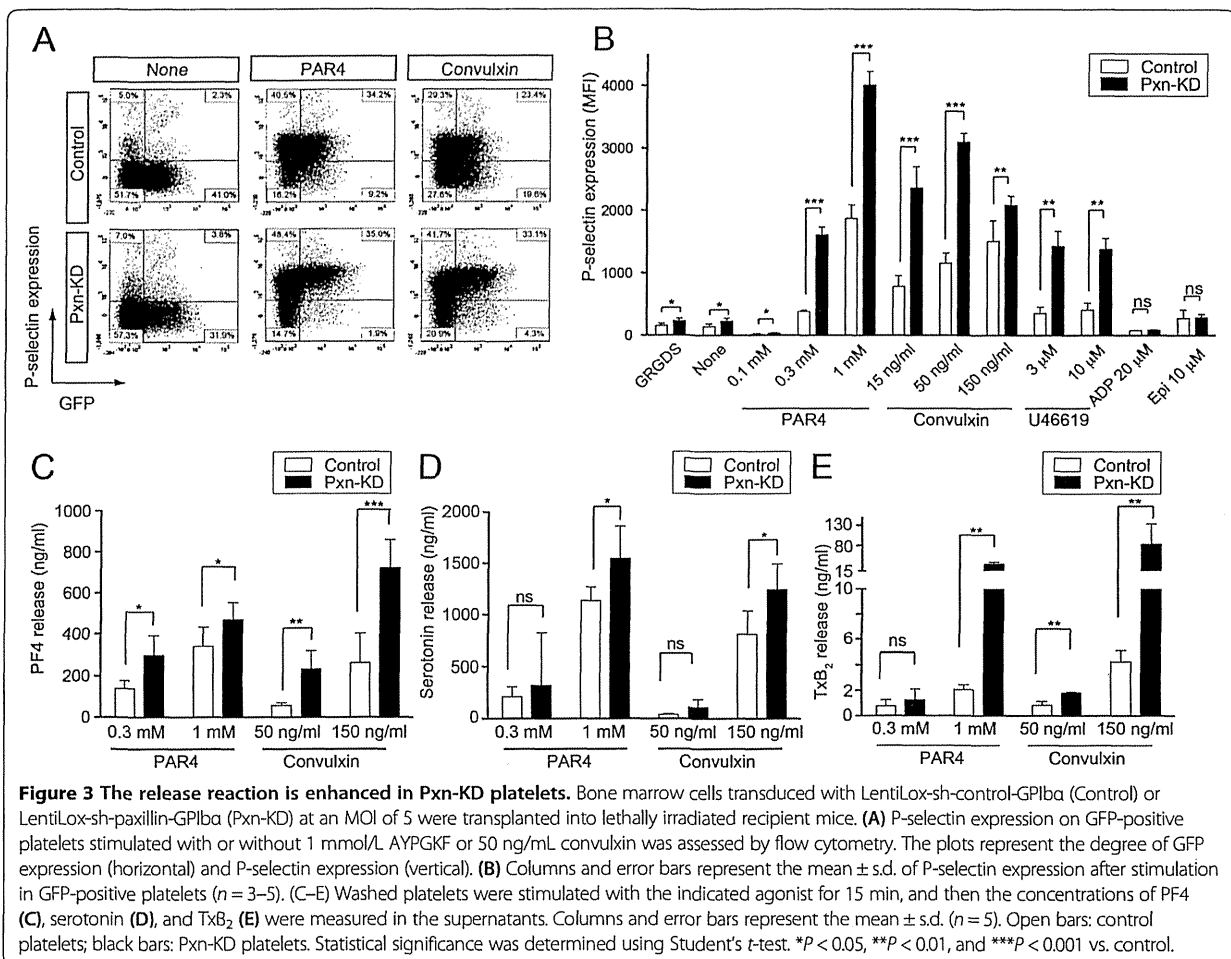
Figure 3 The release reaction is enhanced in Pxn-KD platelets. Bone marrow cells transduced with LentiLox-sh-control-GPIbα (Control) or LentiLox-sh-paxillin-GPIbα (Pxn-KD) at an MOI of 5 were transplanted into lethally irradiated recipient mice. **(A)** P-selectin expression on GFP-positive platelets stimulated with or without 1 mmol/L AYPGKF or 50 ng/mL convulxin was assessed by flow cytometry. The plots represent the degree of GFP expression (horizontal) and P-selectin expression (vertical). **(B)** Columns and error bars represent the mean ± s.d. of P-selectin expression after stimulation in GFP-positive platelets (n = 3–5). (C–E) Washed platelets were stimulated with the indicated agonist for 15 min, and then the concentrations of PF4 **(C)**, serotonin **(D)**, and TxB$_2$ **(E)** were measured in the supernatants. Columns and error bars represent the mean ± s.d. (n = 5). Open bars: control platelets; black bars: Pxn-KD platelets. Statistical significance was determined using Student's t-test. $*P < 0.05$, $**P < 0.01$, and $***P < 0.001$ vs. control.
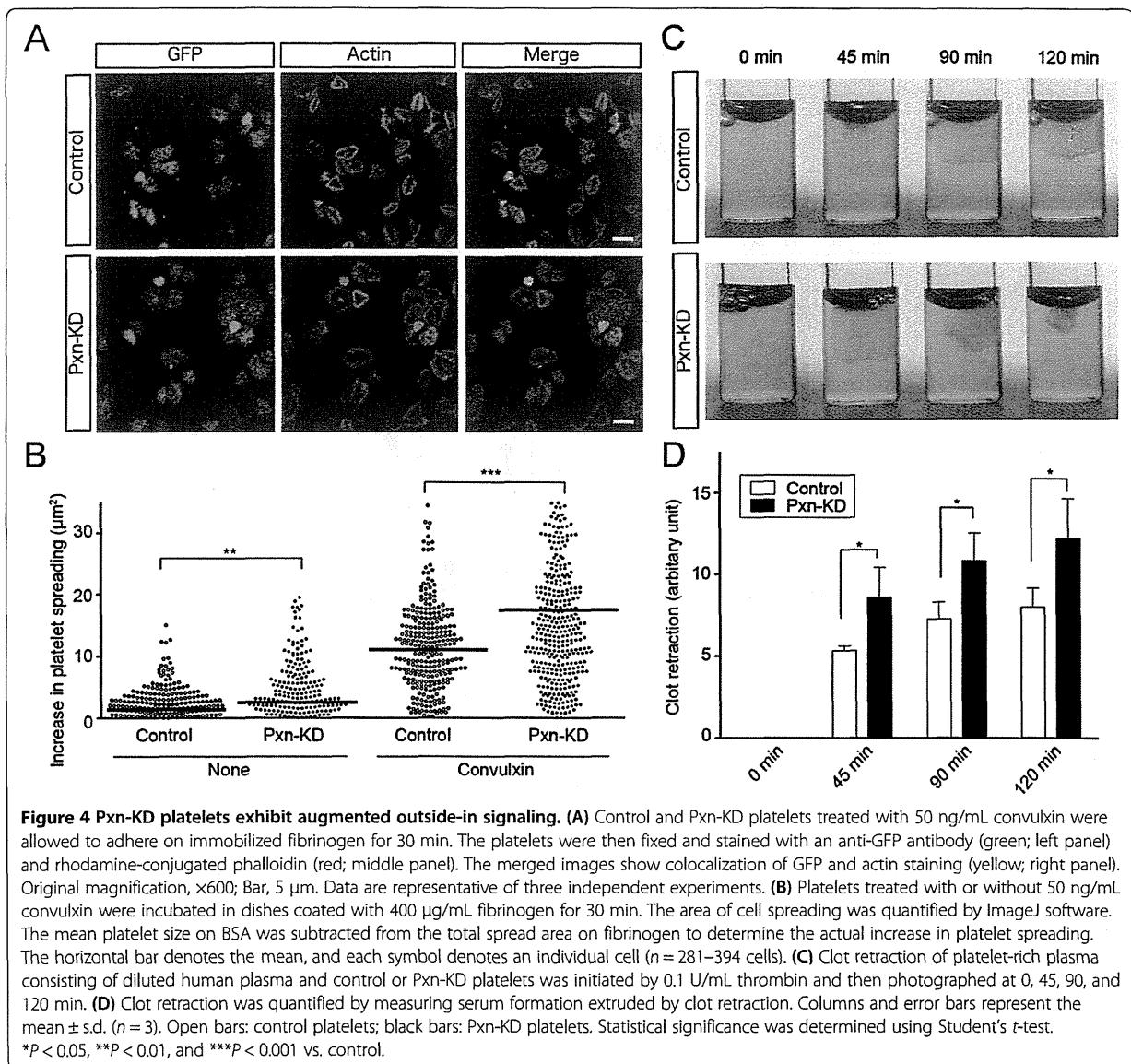
secondary effects of platelet aggregation, influx of extracellular calcium, and release reactions, we preincubated the platelets with EDTA, apyrase, and SQ29548. Intracellular calcium mobilization induced by the GPVI agonist convulxin and G protein-coupled receptor stimulation with AYPGKF was rather decreased by Pxn-KD (Figure 5B). These data suggest that paxillin targets downstream signaling of calcium mobilization or a calcium-independent signaling pathway.

To explore the importance of calcium-independent signaling pathways in Pxn-KD platelets, we employed BAPTA-AM, an intracellular calcium chelator, to exclude the effect of calcium mobilization. Because JON/A requires extracellular calcium for antibody binding, we assessed P-selectin expression induced by an agonist. Pretreatment with BAPTA-AM significantly suppressed P-selectin expression in both control and Pxn-KD platelets (Figure 5C). On the other hand, P-selectin expression elicited by an agonist was still observed in Pxn-KD platelets even in the presence of BAPTA-AM (Figure 5C).

These data indicate that downstream signaling from intracellular calcium mobilization is amplified by Pxn-KD, and the calcium-independent pathway is activated by Pxn-KD to increase platelet activation.

Pxn-KD augments platelet adhesion and thrombus formation in vivo

Finally, we examined the contribution of paxillin to thrombus formation in vivo. To visualize thrombus formation in vivo, we used a direct visual technique based on confocal microscopy in mesenteric capillaries [26]. Thrombus formation in this system was initiated by the production of ROS following laser irradiation [26]. Laser irradiation-induced thrombus formation was significantly enhanced in Pxn-KD platelets (Figure 6A and 6B and Additional files 6 and 7). In addition, there was an enhancement of thrombus formation initiated by FeCl$_3$ in large femoral arteries (Additional file 8). Moreover, bleeding times after tail clipping significantly shortened in Pxn-KD experiments (Figure 6C). These findings support

Figure 4 Pxn-KD platelets exhibit augmented outside-in signaling. (A) Control and Pxn-KD platelets treated with 50 ng/mL convulxin were allowed to adhere on immobilized fibrinogen for 30 min. The platelets were then fixed and stained with an anti-GFP antibody (green; left panel) and rhodamine-conjugated phalloidin (red; middle panel). The merged images show colocalization of GFP and actin staining (yellow; right panel). Original magnification, ×600; Bar, 5 μm. Data are representative of three independent experiments. **(B)** Platelets treated with or without 50 ng/mL convulxin were incubated in dishes coated with 400 μg/mL fibrinogen for 30 min. The area of cell spreading was quantified by ImageJ software. The mean platelet size on BSA was subtracted from the total spread area on fibrinogen to determine the actual increase in platelet spreading. The horizontal bar denotes the mean, and each symbol denotes an individual cell ($n = 281$–394 cells). **(C)** Clot retraction of platelet-rich plasma consisting of diluted human plasma and control or Pxn-KD platelets was initiated by 0.1 U/mL thrombin and then photographed at 0, 45, 90, and 120 min. **(D)** Clot retraction was quantified by measuring serum formation extruded by clot retraction. Columns and error bars represent the mean ± s.d. ($n = 3$). Open bars: control platelets; black bars: Pxn-KD platelets. Statistical significance was determined using Student's t-test. $*P < 0.05$, $**P < 0.01$, and $***P < 0.001$ vs. control.

our hypothesis that paxillin is an important negative regulator of platelet activation and thrombus formation in vivo.

Discussion

Here, we found that the LIM protein paxillin is a negative regulator of platelet activation in mice. The negative regulation of platelet activation by paxillin was not limited to a specific signaling pathway, because Pxn-KD enhanced platelet activation in response to a variety of agonists. We also confirmed that thrombus formation was augmented in Pxn-KD platelets in vivo. This finding is notable because several previous reports suggest that changes in paxillin function actually reduce integrin signaling [13,14]. Furthermore, a previous finding in platelets has

demonstrated the possible role of paxillin as a negative feedback regulator after integrin ligation to regulate the activity of Lyn tyrosine kinase [17]. However, this mode of regulation cannot fully explain the phenotypes of Pxn-KD platelets, because both outside-in and inside-out signaling were augmented by Pxn-KD. Our results reveal a new cellular function of paxillin and indicate new mechanisms that modulate platelet activation.

The most interesting result of this study was that Pxn-KD significantly enhanced the upstream signaling pathways that converge on platelet activation. Appropriate inhibition of the platelet response is essential to control pathological thrombus formation. It is well known that the mediators that enhance intracellular cAMP or cGMP
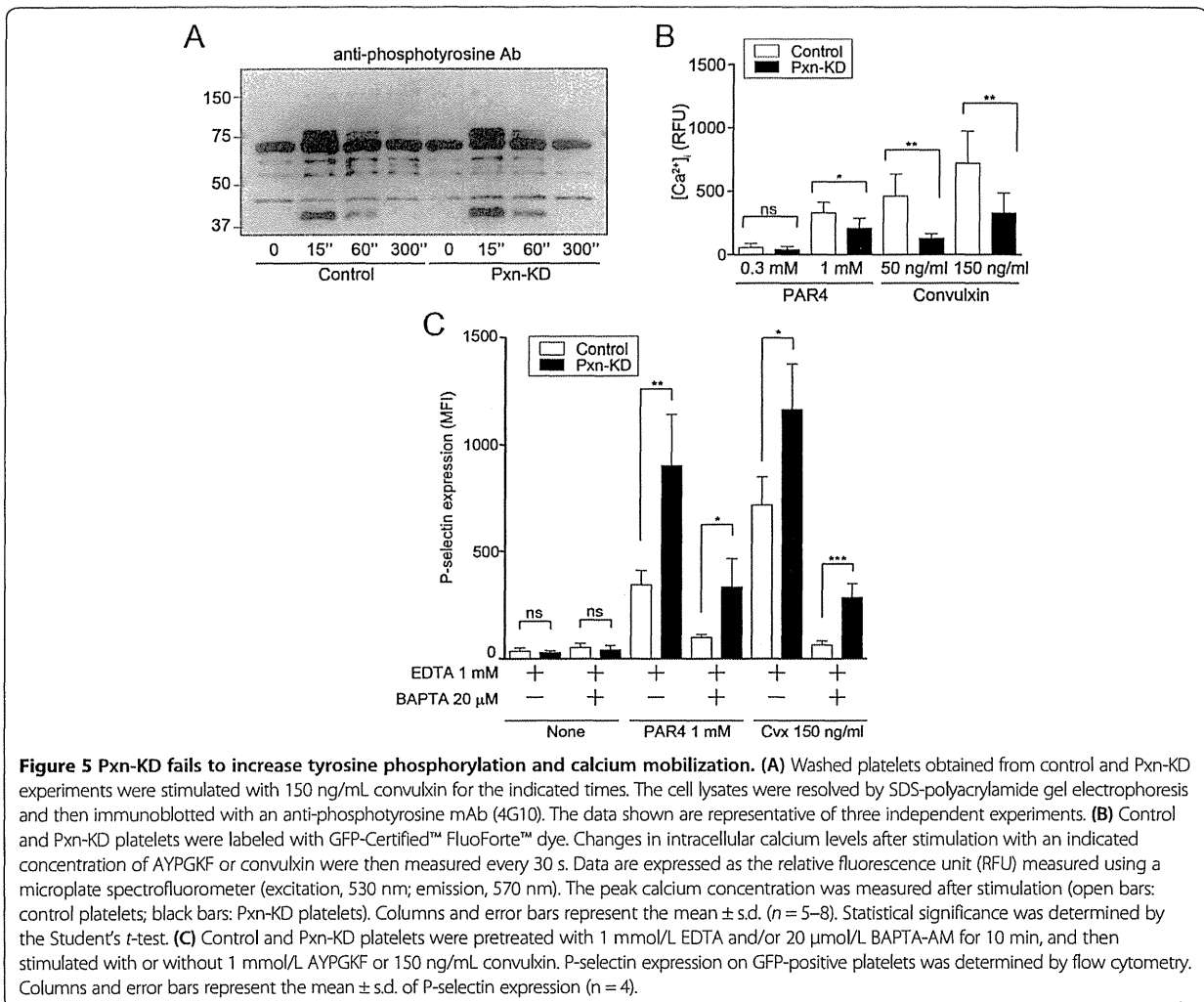
Figure 5 Pxn-KD fails to increase tyrosine phosphorylation and calcium mobilization. (A) Washed platelets obtained from control and Pxn-KD experiments were stimulated with 150 ng/mL convulxin for the indicated times. The cell lysates were resolved by SDS-polyacrylamide gel electrophoresis and then immunoblotted with an anti-phosphotyrosine mAb (4G10). The data shown are representative of three independent experiments. **(B)** Control and Pxn-KD platelets were labeled with GFP-Certified™ FluoForte™ dye. Changes in intracellular calcium levels after stimulation with an indicated concentration of AYPGKF or convulxin were then measured every 30 s. Data are expressed as the relative fluorescence unit (RFU) measured using a microplate spectrofluorometer (excitation, 530 nm; emission, 570 nm). The peak calcium concentration was measured after stimulation (open bars: control platelets; black bars: Pxn-KD platelets). Columns and error bars represent the mean ± s.d. (n = 5–8). Statistical significance was determined by the Student's t-test. **(C)** Control and Pxn-KD platelets were pretreated with 1 mmol/L EDTA and/or 20 μmol/L BAPTA-AM for 10 min, and then stimulated with or without 1 mmol/L AYPGKF or 150 ng/mL convulxin. P-selectin expression on GFP-positive platelets was determined by flow cytometry. Columns and error bars represent the mean ± s.d. of P-selectin expression (n = 4).

levels, including prostacyclin, prostaglandin E_1, and nitric oxide, are strong extrinsic inhibitors of platelet activation [27]. These extrinsic mediators ameliorate the broad platelet activation elicited by various agonists [27]. Intrinsic negative regulators of platelet activation have been identified recently, but many of these proteins only control a specific receptor signaling pathway. GPVI-mediated immunoreceptor tyrosine-based activation motif (ITAM) signaling is regulated by immunotyrosine-based inhibitory motif (ITIM)-containing receptors including platelet endothelial cell adhesion molecule 1 and carcinoembryonic antigen-related cell adhesion molecule 1 [28,29]. Furthermore, Lyn tyrosine kinase has been reported to inhibit ITAM signaling by inducing tyrosine phosphorylation of ITIM [28]. It has also been reported that binding of a regulator of G-protein signaling to the Giα subunit limits platelet responsiveness to the receptor, which is independent of Rap1b [30]. Conversely, paxillin may downregulate platelet activity by modulating a common pathway,

because Pxn-KD resulted in marked platelet hyperactivation in response to stimulation of tyrosine phosphorylation-based receptors and G protein-coupled receptors.

Although paxillin is reportedly involved in various integrin-mediated cellular functions, many of these functions are limited to outside-in signaling pathways. Paxillin-deficient embryos show embryonic lethality, and the phenotype closely resembles that of fibronectin-deficient mice [31]. Moreover, paxillin-deficient fibroblasts show reductions in cell migration and tyrosine phosphorylation following cell adhesion [31]. Chimeric integrin αIIbβ3 with a cytoplasmic tail substitution of α4β1 or α9β1, which facilitates paxillin binding, significantly inhibits cell spreading, but does not affect αIIbβ3-dependent cell adhesion [18,19]. Inhibition of paxillin binding to integrin α4 inhibits leukocyte recruitment to an inflammatory site [32]. These data suggest important roles of paxillin in outside-in signaling by direct interaction with the integrin α-subunit. However, in this study, inside-out and outside-